Published in final edited form as:

Neuropeptides. 2018 April ; 68: 57–74. doi:10.1016/j.npep.2018.02.003.

Determination of neurotensin projections to the ventral tegmental area in mice

Hillary L. Woodworth[a], **Juliette A. Brown**[b], **Hannah M. Batchelor**[a], **Raluca Bugescu**[a], **Gina M. Leinninger**[a,*]

[a]Department of Physiology, Michigan State University, East Lansing, MI, USA

[b]Department of Pharmacology and Toxicology, Michigan State University, East Lansing, MI, USA

Abstract

Pharmacologic treatment with the neuropeptide neurotensin (Nts) modifies motivated behaviors such as feeding, locomotor activity, and reproduction. Dopamine (DA) neurons of the ventral tegmental area (VTA) control these behaviors, and Nts directly modulates the activity of DA neurons via Nts receptor-1. While Nts sources to the VTA have been described in starlings and rats, the endogenous sources of Nts to the VTA of mice remain incompletely understood, impeding determination of which Nts circuits orchestrate specific behaviors in this model. To overcome this obstacle we injected the retrograde tracer Fluoro-Gold into the VTA of mice that express GFP in Nts neurons. Identification of GFP-Nts cells that accumulate Fluoro-Gold revealed the Nts afferents to the VTA in mice. Similar to rats, most Nts afferents to the VTA of mice arise from the medial and lateral preoptic areas (POA) and the lateral hypothalamic area (LHA), brain regions that are critical for coordination of feeding and reproduction. Additionally, the VTA receives dense input from Nts neurons in the nucleus accumbens shell (NAsh) of mice, and minor Nts projections from the amygdala and periaqueductal gray area. Collectively, our data reveal multiple populations of Nts neurons that provide direct afferents to the VTA and which may regulate specific aspects of motivated behavior. This work lays the foundation for understanding endogenous Nts actions in the VTA, and how circuit-specific Nts modulation may be useful to correct motivational and affective deficits in neuropsychiatric disease.

Keywords

Lateral hypothalamic area; Preoptic area; Nucleus accumbens; Retrograde tracing; Fluoro-Gold; Motivation; Reward; Dopamine

1. Introduction

Neurotensin (Nts) is a 13 amino-acid neuropeptide that was first extracted from the bovine hypothalamus (Carraway and Leeman, 1973). Nts has subsequently been identified throughout the brain (Beck et al., 1989; Carraway and Leeman, 1976; Jennes et al., 1982;

*Corresponding author at: Department of Physiology, Michigan State University, 567 Wilson Rd, BPS Bldg, Room 3183, East Lansing, MI 48824, USA. leinning@msu.edu (G.M. Leinninger).

Kitabgi et al., 1990; Uhl et al., 1979) and has been implicated in regulating a diverse repertoire of physiology and motivated behaviors including feeding, locomotor activity, social behavior, analgesia, sleep, and response to addictive drugs (Boules et al., 2011; Brown et al., 2017; Cape et al., 2000; Demeule et al., 2014; Ferraro et al., 2016; Fitzpatrick et al., 2012; Gammie et al., 2009; Merullo et al., 2015b; Smith et al., 2012). Nts may direct certain behaviors via actions in the ventral tegmental area (VTA), based on findings that different types of VTA neurons orchestrate distinct goal-directed behaviors (Lammel et al., 2012; Stamatakis et al., 2013; van Zessen et al., 2012), and that a specific subset of VTA neurons expresses neurotensin receptor-1 (Woodworth et al., 2017a). The VTA is predominantly comprised of dopamine (DA) neurons that project to and release DA in the nucleus accumbens (NA), prefrontal cortex (PFC), hippocampus, or amygdala to modify goal-directed behaviors (for review see Bromberg-Martin et al., 2010; Salamone and Correa, 2012). In contrast, the caudal “tail” of the VTA that forms a continuum with the rostromedial tegmental nucleus (RMTg) is enriched with GABA-ergic neurons, which inhibit VTA DA neurons and serve as negative regulators of DA-mediated behaviors (Carr and Sesack, 2000; Margolis et al., 2012; Tan et al., 2012; van Zessen et al., 2012). Given that alterations in both VTA DA and Nts signaling have been implicated in the pathogenesis of drug addiction, depression, anxiety, schizophrenia, autism, pain processing and obesity, there is likely functional overlap of these systems (Boules et al., 2014; Caceda et al., 2012; Carey et al., 2017; Ellenbroek et al., 2016; Ferraro et al., 2016; Fitzpatrick et al., 2012; Howes et al., 2017; Kim and Mizuno, 2010; Li et al., 2016; Nestler and Carlezon Jr, 2006; Rothwell, 2016; Theoharides et al., 2016; Volkow et al., 2013). It is therefore critical to define the precise neural mechanisms by which Nts engages the VTA, to understand how it regulates such diverse physiology and how Nts signaling becomes maladaptive in disease.

Pharmacologic Nts activates VTA DA neurons (Legault et al., 2002; Seutin et al., 1989; Sotty et al., 2000, 1998; St-Gelais et al., 2004; Werkman et al., 2000), thereby increasing DA release in the NA (Kalivas et al., 1983; Kalivas and Duffy, 1990; Sotty et al., 2000, 1998; Steinberg et al., 1995) that can modify goal directed behaviors. Indeed, intra-VTA Nts has been shown to suppress homeostatic and motivated feeding (Cador et al., 1986; Kelley et al., 1989), increase locomotor activity (Cador et al., 1986; Elliott and Nemeroff, 1986; Feifel and Reza, 1999; Kalivas et al., 1983; Kalivas and Duffy, 1990; Kalivas et al., 1981; Panayi et al., 2005; Steinberg et al., 1994) and support self-administration (Glimcher et al., 1987; Kempadoo et al., 2013; Rompre and Gratton, 1993), conditioned place preference (CPP) (Glimcher et al., 1984; Rouibi et al., 2015) and locomotor sensitization similar to addictive drugs (Elliott and Nemeroff, 1986; Kalivas and Duffy, 1990; Kalivas and Taylor, 1985; Voyer et al., 2017). Intriguingly, many of these behavioral effects are specific to the VTA because Nts administration outside of the VTA elicits different effects. For example, while Nts injection in the VTA increases locomotor activity and DA release, intra-NA or central Nts decreases locomotor activity and does not alter DA release (Elliott et al., 1986; Kalivas et al., 1983, 1984; Meisenberg and Simmons, 1985; Vadnie et al., 2014; van Wimersma Greidanus et al., 1984). Similarly, intra-VTA Nts does not alter acute locomotor response to psychostimulants (Elliott and Nemeroff, 1986), whereas ICV or intra-NA Nts reduces psychostimulant or DA-induced hyperactivity (Ervin et al., 1981; Jolicoeur et al., 1985; Nemeroff et al., 1983; Sarhan et al., 1997; Skoog et al., 1986). One notable exception to this

is Nts-mediated suppression of feeding behavior, as both central and direct administration of Nts in the VTA suppress feeding in fasted and satiated animals (Cador et al., 1986; Cooke et al., 2009; Luttinger et al., 1982). Taken together, these data suggest that there must be projection-specified populations of Nts neurons, only some of which project to the VTA to coordinate motivated locomotor and reward behaviors.

It is clear that exogenous Nts impacts the mesolimbic DA system, yet the endogenous sources of Nts to the VTA have yet to be fully characterized. Furthermore, defining Nts inputs to the VTA across species is important to determine how this neuropeptide modulates DA-mediated behaviors relevant to animal survival. For example, European starlings exhibit Nts immunoreactivity within the VTA, at least some of which originates from the preoptic area (POA); this starling Nts POA → VTA circuit is implicated in regulating sexually-motivated singing behavior (Merullo et al., 2015a, b). Zahm and colleagues have characterized endogenous sources of Nts to the VTA in rats (Geisler and Zahm, 2006a,b; Zahm et al., 2001). Abundant Nts-immunoreactive terminals are found within the VTA of rats (Beaudet and Woulfe, 1992; Hokfelt et al., 1984; Szigethy and Beaudet, 1989; Woulfe and Beaudet, 1989) and in mice, where they are found in close opposition to VTA DA neurons (Opland et al., 2013), indicating that some Nts is released to the VTA. Nts afferents to the VTA were examined in rats by injecting the retrograde tracers Fluoro-Gold (FG) and the cholera toxin beta subunit (CTb) into the VTA and using in situ hybridization (ISH) to label Nts cell bodies, demonstrating that most Nts inputs to the VTA originate from the preoptic area (POA) and rostral lateral hypothalamic area (LHA) (Zahm et al., 2001). Yet, lesioning the POA and LHA in rats does not substantially reduce Nts terminals in the VTA, suggesting there may be other important sources of endogenous input in this species (Geisler and Zahm, 2006b). Indeed, injection of a wheat germ agglutinin transynaptic tracer (WGA-apoHRP-gold) into the VTA of rats confirmed afferents from the POA and LHA, and identified putative afferents from the NA shell (NAsh), dorsal raphe (DR), ventral endoprifirom area, lateral septum (LS), pedunculopontine tegmental nucleus (PTg), and laterodorsal tegmental nucleus (LDTg) (Geisler and Zahm, 2006a).

In comparison with starlings and rats, the Nts system in mice has been comparatively little studied, and so the sources of endogenous mouse Nts input to the VTA remain incompletely understood. Studies across species were limited by the inability to easily identify Nts-expressing cells, but the recent development of Nts^{Cre} mice enables the facile detection and manipulation of mouse Nts neurons using Cre-Lox technology. Using these mice we have identified a large population of Nts neurons in the LHA that project to the VTA, consistent with the prior afferent mapping done in rats, and manipulation of these LHA Nts neurons reveals their crucial contributions to motivated behavior and energy balance (Brown et al., 2017; Leinninger et al., 2011; Opland et al., 2013; Patterson et al., 2015; Woodworth et al., 2017b). The LHA may be just one of several sites by which Nts orchestrates distinct behavioral responses in the mouse VTA, thus it will be important to define all Nts afferents to the VTA and test their roles individually. Indeed, Nts^{Cre} mice were recently used to define how medial preoptic area Nts neurons projecting to the VTA mediate social reward behavior, but this projection does not modify feeding (McHenry et al., 2017). Since these data suggest that distinct sources of mouse Nts coordinate specific DA-mediated behaviors relevant to survival (e.g. feeding vs. social behavior/mating), it is imperative to define and

then to systematically test specific Nts → VTA circuits to understand their contributions to physiology and behavior. The prior literature characterizing the rat Nts system has served as a guide for mouse studies, but mice and rats differ in Nts expression (Smits et al., 2004), so they may also differ in the distribution of Nts afferents to the VTA. Thus, herein we defined the mouse Nts neurons that project to the VTA by injecting the retrograde tracer FG into the VTA of *Nts*^{Cre}*;GFP* reporter mice, permitting robust, simultaneous detection of Nts neurons and VTA afferents.

2. Materials and methods

2.1. Animals

Mice were bred and housed in a 12 h light/12 h dark cycle and cared for by Campus Animal Resources (CAR) at Michigan State University. Animals had ad lib access to chow (Teklad 7913) and water. All animal protocols were approved by the Institutional Animal Care and Use Committee (IACUC) at Michigan State University, in accordance with Association for Assessment and Accreditation of Laboratory Animal Care and National Institutes of Health guidelines.

Nts^{Cre} mice (Leinninger et al., 2011) [Jackson stock # 017525], were bred to wild-type C57/Bl6 mice for seven generations to obtain fully backcrossed animals. To visualize Nts neurons, heterozygous *Nts*^{Cre} mice were crossed with homozygous *Rosa26*$^{EGFP\text{-}L10a}$ mice (Krashes et al., 2014), and progeny heterozygous for both *Nts*^{Cre} and *Rosa26*^{EGFP}*-L10a* alleles were studied (referred to as *Nts*^{Cre};*GFP* mice). Genotyping was performed using standard PCR using the following primer sequences: *Nts*^{Cre}: common forward: 5′ ATA GGC TGC TGA ACC AGG AA, cre reverse: 5′ CCA AAA GAC GGC AAT ATG GT and WT reverse: 5′ CAA TCA CAA TCA CAG GTC AAG AA. *Rosa26*$^{EGFP\text{-}L10a}$: mutant forward: 5′ TCT ACA AAT GTG GTA GAT CCA GGC, WT forward: 5′ GAG GGG AGT GTT GCA ATA CC and common reverse: 5′ CAG ATG ACT ACC TAT CCT CCC. Adult male and female *Nts*^{Cre}*;GFP* mice (ages 15–26 wk) were used for all studies.

2.2. Colchicine treatment

Stereotaxic surgeries were performed as described previously (Brown et al., 2017). Briefly, adult *Nts*^{Cre}*;GFP* mice received a pre-surgical injection of carprofen (5 mg/kg *s.c.*) and were anesthetized with 3–4% isoflurane/O_2 in an induction chamber before being placed into a mouse stereotaxic frame (Kopf). Under 1–2% inhaled isoflurane, an access hole was drilled in the skull and a guide cannula with stylet extending 0.5 mm below the cannula (PlasticsOne) was lowered into the right lateral ventricle, in accordance with the mouse brain atlas (Keith and Franklin, 2007) (A/P: −0.30 mm, M/L: −1.00 mm, D/V: −2.1 mm from Bregma). The stylet was then removed from the guide cannula and replaced with an injector that extended 0.5 mm beyond the end of the cannula. The injector was fitted with tubing attached to a Hamilton syringe, which was used to deliver 250 nL of colchicine (Sigma, 40 μg/μL) into the lateral ventricle at a rate of 100 nL/min. After 5 min the injector was removed, and the cannula was raised out of the ventricle. The access hole in the skull was filled with bone wax and the incision was closed using VetBond surgical adhesive. Mice

were individually housed for 2 days to permit the colchicine to inhibit axonal transport, then were perfused with 10% neutral buffered formalin.

2.3. Fluoro-Gold (FG) injections

Adult *Nts*^{Cre}*;GFP* mice were anesthetized and fitted into a stereotaxic frame as described above. An access hole was drilled into the skull, through which a guide cannula containing a stylet extending 1 mm below the cannula (PlasticsOne) was lowered unilaterally into the VTA in accordance with the mouse brain atlas (Keith and Franklin, 2007) (A/P: −3.2 mm, M/L: −0.48 mm, D/V: −4.6 mm from Bregma). The stylet was then replaced with a similar length injector that was attached to a Hamilton syringe, via which 15 nL of FG was injected into the VTA over 30 s. After 5 min the injector was removed, the cannula was raised out of the VTA, and the incision was closed as described above. Mice were then individually housed for 7 days to allow for axonal transport of FG to cell bodies, at which point they were perfused with 10% neutral buffered formalin.

In general, mice were included in the study if the FG injection was targeted to and confined within the VTA, and if FG-labeled neurons were observed in a pattern consistent with mouse VTA afferents based on prior studies that separately labeled afferents to VTA DA, GABA and glutamate neurons (Faget et al., 2016; Watabe-Uchida et al., 2012). As a first step to recognizing such mice, we identified the injection site via the scarring and/or autofluoresence that accompanies tissue disruption along the injection tract, then we examined potential FG spread around these sites. There is no direct mechanism to visualize injected FG or to verify FG spread, but we noted that injection caused tissue around the injection site to be brighter in appearance compared to the un-injected contralateral side. We mapped the extent of this “bright” tissue in each mouse as an approximation of FG spread, represented by the magenta areas mapped onto the mouse brain atlas in Fig. 2B–F. Via this analysis we identified cases in which injections were centered within (e.g. cases F23, F27, F29) or just outside of the VTA (such as case F19, Fig. 2B), and in which the apparent FG spread encompassed the VTA. In one case (F28, Fig. 2E) we could not identify the precise injection site, which may have fallen outside of the series of sections we analyzed, but we did observe tissue brightness on the injected side that was used to map the approximate FG spread.

Next we sought to include only cases in which the FG was primarily contained within the VTA and had not spread laterally to the substantia nigra compacta (SN), as neurons within the VTA and SN have very different functions. We therefore used the retrograde tracing atlas generated by Watabe-Uchida et al. as a secondary method to discriminate cases with FG injection primarily targeted within the VTA vs. those in which FG had also spread to the SN (Watabe-Uchida et al., 2012). Their work established that VTA DA neurons (which comprise the majority of VTA neurons) receive dense projections from the LHA, but SN DA neurons receive comparably few afferents from the LHA. Furthermore, SN DA neurons receive significant inputs from the caudate/putamen (CPu) portion of the dorsal striatum (DS) at approximate Bregma level − 1.70 mm (Keith and Franklin, 2007)), but VTA DA generally neurons do not. Additionally, VTA neurons receive substantial input from the NA, while the SN receives preferential input from the CPu portion of the DS at the same bregma

level (+1.10 to +1.90). Based on these findings, we reasoned that a FG injection primarily confined within the VTA, without spread to the SN, would result in numerous FG-labeled cell bodies within the LHA and NA but few within the DS (Fig. 2G and data not shown for the NA and DS from +1.10–1.90). We therefore only included mice for this study that met all of the following criteria: 1) the FG injection and apparent spread was within the vicinity of the VTA (Fig. 2B–F, magenta shading), 2) numerous FG-labeled cell bodies were observed within the LHA and NA, consistent with the established LHA → VTA and NA → VTA projections and 3) absence of FG-labeled cell bodies within the DS that would suggest FG spread to the SN, consistent with the established DS → SN projection (Watabe-Uchida et al., 2012, Faget et al., 2016). Out of 10 FG-injected *Nts*^{Cre}*;GFP* mice, 5 were excluded from analysis because the injection was targeted lateral or dorsal to the VTA and/or the pattern of FG-labeled neurons was more consistent with SN rather than VTA afferents. In one case (F29, Fig. 2F) we noted significant autofluoresence that raised concern about potential FG leak along the injection tract, but secondary analysis revealed retrograde tracing consistent with VTA-targeting without any extensive labeling to other sites. We concluded that this autofluoresence was due to low-level inflammation, and did not preclude afferent analysis from this case.

2.4. Perfusions and immunohistochemistry

Colchicine or FG-injected *Nts*^{cre}*;GFP* mice were deeply anesthetized with sodium pentobarbital, transcardially perfused with 10% formalin and brains were post-fixed for 24 h. After dehydration with 30% sucrose the brains were coronally sectioned (30 μm) using a freezing microtome (Leica). Each brain was sectioned into four separate but equally represented series. Immunofluorescence was performed as previously described (Leinninger et al., 2011). Sections were incubated with chicken anti-GFP (1:2000, Abcam) and mouse anti-tyrosine hydroxylase (TH) (1:1000, Millipore) or rabbit anti-Fluoro-Gold (1:500, Fluoro-Gold chrome) followed by incubation with a 1:200 solution containing species-specific secondary antibodies with fluorescent conjugates (Alexa Fluor® 488 AffiniPure donkey anti-chicken – Jackson ImmunoResearch, ab13970; donkey anti-rabbit IgG (H + L) Highly Cross Adsorbed Secondary Antibody Alexa Fluor® 568 – ThermoFisher Scientific, A10042; donkey anti-mouse IgG (H + L) Highly Cross Adsorbed Secondary Antibody, Alexa Fluor® 568- ThermoFisher Scientific, A10037).

2.5. Imaging and quantification

One of the four coronal series of brain sections from each mouse was analyzed in these studies to determine the number of colocalized neurons throughout all regions of the brain (see Table 1 for abbreviations of the brain structures referenced herein). This is a conservative quantification method sufficient to compare relative neuronal abundance between different brain areas, without oversampling that might occur if counts were multiplied by 4 to approximate the number of cells throughout the entire brain. Brain sections were analyzed using an Olympus BX53 fluorescence microscope outfitted with FITC and Texas Red filters. Microscope images were collected using Cell Sens software and a Qi-Click 12 Bit cooled camera, and images were analyzed using Photoshop software (Adobe). For quantification of Nts neurons in the VTA, four representative coronal sections

across similar bregma coordinates from each animal were assessed for number of Nts neurons and colocalization with TH.

Although we observed substantial numbers of GFP-labeled Nts neurons and FG-labeled neurons throughout the brain, only a few regions were found to contain colocalized neurons, henceforth referred to as Nts/FG+ neurons. We therefore counted the number of colocalized neurons in these regions. For each of the 5 well-targeted FG animals, multiple 10× images were captured of each brain section and were assigned a bregma coordinate based on the mouse brain atlas (Keith and Franklin, 2007). We chose 10× magnification because most brain areas of interest can be captured in a single 10× image, which allowed us to use multiple landmarks within the image to define region borders. 10× images spanning the entire rostrocaudal axis of a particular brain area containing Nts/FG+ neurons were then compiled using Photoshop, so that images from each animal were arranged side-by-side according to bregma level. The atlas was used to identify pertinent landmarks, and the borders of each anatomical area were digitally drawn onto each image. Once anatomical boundaries were defined, the number of GFP/FG+ double-positive neurons were counted by digitally magnifying the 10× images in Photoshop to 20× or higher. To improve visualization of FG+ neurons, a contrast mask of +100 was applied globally to each image for quantification. These images were used to identify, mark and count the number of Nts/FG+ neurons. A neuron was considered to contain co-localized GFP and FG+ by the following criteria: 1) FG immunoreactivity filled the same physical area occupied by GFP, 2) FG immunoreactivity was not present outside the boundary of GFP immunoreactivity and 3) the pattern of FG and GFP immunoreactivity shared common overlapping features including similarly shaped soma size, processes and nuclear void. Because GFP typically fills the soma and processes, whereas FG tended to accumulate in the soma only, lack of FG immunoreactivity in processes did not count as exclusion criteria. To facilitate clarity of neuronal features in figures depicting FG+ neurons, they have been digitally enhanced in Photoshop to improve contrast and, in some cases, brightness. Fig. 3 schematizes the distribution of Nts/FG+ neurons found in each brain region, Table 2 depicts the relative density of these afferents, and Fig. 4 reports the total number of Nts/FG+ neurons counted from each region, which represents approximately ¼ of the entire brain. We did not multiply our Nts/FG+ neuron counts by 4 to estimate total cells in each region throughout the whole brain, due to concerns that this could introduce oversampling error for smaller nuclei. To assess the relative density of Nts afferents to the VTA arising from brain regions, the total number of Nts/FG+ cells in a region was divided by the number of counted sections containing the region (Table 2).

3. Results

3.1. Validation of Nts^{Cre};GFP mice to identify Nts neurons

We bred mice expressing Cre-recombinase in Nts neurons (Leinninger et al., 2011) to a Cre-inducible L10-eGFP reporter (Krashes et al., 2014), producing progeny that express GFP selectively in Nts neurons (we refer to these as *Nts^{Cre};GFP* mice). To investigate whether this line faithfully identifies Nts-expressing cells (Fig. 1) we treated *Nts^{Cre};GFP* mice with colchicine and examined GFP and Nts immunoreactivity (Nts-IR). We focused our

assessment on three brain areas known to contain significant populations of Nts-expressing cells as confirmed via ISH (Lein et al., 2007): the LHA, POA and NA. Essentially all of the Nts-IR cells in these regions colocalize with GFP, and GFP cells largely overlapped with Nts-IR, confirming that the *Nts^{Cre};GFP* line correctly identifies Nts neurons. A minor population of GFP cells were noted that did not contain observable Nts-IR. Our data concur with a recent report of dual-label ISH in the *Nts^{Cre}* line, which showed almost complete overlap of *Nts* and *Cre* (McHenry et al., 2017). Taken together, these data verify the fidelity of the *Nts^{Cre};GFP* mouse line and its usefulness to identify and study Nts neurons.

3.2. Characterization of Nts neurons that project to the VTA

To identify all Nts neurons that project to or through the VTA, we stereotaxically injected *Nts^{Cre};GFP* mice with the retrograde tracer FG, which is taken up by local terminals as well as any damaged axons of passage at the injection site. Any cell body found to contain both FG (magenta) and GFP (green) represents an Nts neuron that projects to or through the VTA (grey) (Fig. 2A). We verified VTA targeting by mapping the locations of the midbrain injection tracts and by carefully assessing FG labeling within brain regions known to preferentially project to the DA neurons of the VTA vs. the SN, based on the previous work of Watabe-Uchida (Watabe-Uchida et al., 2012). The LHA and NA provide substantial inputs to the DA neurons of VTA but far fewer to those in the SN; thus, we reasoned that VTA-targeting should result in substantial FG-labeled cell bodies in the LHA and NA, warranting inclusion in our study. Since the dorsal striatum (DS) provides significantly more input to the SN vs. the VTA, we further reasoned that any case with robust FG labeling in the DS would indicate FG spillage to the SN and should be excluded from our current VTA-focused inquiry (Fig. 2G and data not shown for NA). Out of 10 animals injected with FG, 5 had injection sites within the VTA and had many FG-labeled neurons in the LHA and NA, but not the DS (Fig. 2B–F); these 5 mice were subsequently analyzed to define Nts afferents to the VTA. Although the injection tracts of cases F19 and F29 appeared on the lateral border of the VTA, these mice were included for analysis because their FG expression was consistent with VTA rather than SN targeting (e.g. robust FG+ labeling in the LHA and NA, with minimal FG+ neurons in the DS). We examined the whole brain of each of the VTA-targeted cases to identify all sources of Nts afferents to the VTA. While our analysis revealed substantial numbers of GFP-labeled Nts neurons and FG-labeled neurons throughout the brain, we only report the brain regions containing colocalized neurons, henceforth referred to as Nts/FG+ neurons. These findings are qualitatively summarized in Fig. 3, and are quantitatively summarized in Fig. 4 and Table 2. Data from individual brain regions are shown in Figs. 5–12.

3.3. Striatum and septum

We observed many Nts/FG+ neurons in the NA shell (NAsh) between +1.75 and 0.85 bregma, but few Nts/FG+ in the NA core (Figs. 4 and 5B). The Nts/FG+ neurons were found within a diffuse continuous band across the rostrocaudal axis of the NAsh, with no clear localization to rostral or caudal regions (Fig. 5B and Table 2). GFP-labeled neurons were also abundant in the olfactory tubercle (OFT), but few were FG+ (Fig. 5C). Compared to the ventral striatum (NA and OFT), the dorsal striatum contained relatively few Nts neurons, which clustered around the lateral and medial borders of the CPu (Fig. 5D, E). We observed

some FG+ neurons in the ventral CPu between +1.94 and 0.62 bregma, but the vast majority did not colocalize with GFP (Fig. 5D). While Nts neurons were abundant in the LS, there were few FG+ neurons (Fig. 5E), and we observed ≤1 Nts/FG+ neuron per coronal section in the LS of mice.

3.4. Cortex and amygdala

The neocortex contained relatively few GFP-labeled Nts neurons with the exception of a prominent band of Nts neurons in the prefrontal cortex (PFC). We noted distinct populations of FG-labeled or Nts neurons in separate layers of the PFC and the lateral orbital cortex (LO), but no Nts/FG+ neurons (Fig. 6B, C). Examination of the amygdala revealed FG-labeled neurons in the central amygdala (CeA) and extended amygdala (EA) with relatively few in the basolateral amygdala (BLA). We detected a concentrated area of Nts neurons in the CeA of mice, which were more numerous in the lateral division in caudal sections (Fig. 6D). Some of these CeA Nts neurons project to the VTA, and were predominantly found between −1.30 and −0.80 bregma (Fig. 6E), although they provide a modest density of projections compared to other sources of Nts input to the VTA (Table 2). A smaller population of Nts/FG+ neurons was observed in the EA.

3.5. IPAC, pallidum and stria terminalis

We noted a few Nts/FG+ neurons in the interstitial nucleus of the posterior limb of the anterior commissure (IPAC), which appeared to represent a caudal extension of the Nts/FG+ neurons described in the NAsh (Fig. 7B), By contrast, Nts expression was consistently scarce in the adjacent ventral pallidum (VP) (Fig. 6B–C), with few Nts/FG+ neurons in the VP near the border with the LPO (Fig. 4). We identified a few Nts/FG+ neurons in the ST of mice, but also many cells containing only Nts or FG+ (Fig. 7C).

3.6. Hypothalamus and adjacent regions

The zona incerta (ZI) runs along the dorsal border of the LHA, and while it contained minimal Nts neurons, many of them were Nts/FG+ (Fig. 8B). Our examination also revealed a dense population of Nts neurons in the neighboring subthalamic nucleus (STN) (Fig. 8C), but we did not observe FG in them. However, the sparse ZI Nts neurons and the abundant STN Nts neurons in the *Nts*^{Cre}*;GFP* mice were consistent with the distribution of *Nts*-positive neurons in these areas reported in the mouse Allen Brain Atlas (Lein et al., 2007).

Within the hypothalamus, the POA provided a large number of Nts afferents to the VTA, whose distribution varied along the rostro-caudal axis. In the caudal POA, the Nts population was most dense in the medial preoptic area (MPO) adjacent to the third ventricle. Many Nts/FG+ neurons were found in the MPO (Fig. 9B) and these VTA-projecting neurons formed a dense cluster centered between −0.22 and +0.02 bregma. In the rostral POA the Nts population was sparse in the MPO but dense within the lateral preoptic area (LPO), where we observed many Nts/FG+ neurons (Fig. 9C) spanning between −0.10 and +0.40 bregma. More caudally in the hypothalamus, the LHA contained a sizeable population of Nts neurons between −1.30 to −1.70 bregma, many of which were labeled with FG from the VTA (Fig. 10B). Compared to the LHA, other hypothalamic sub-regions

contained more sparse populations of Nts neurons, including the dorsomedial hypothalamus (DMH), ventromedial hypothalamus (VMH), arcuate nucleus (ARC), and paraventricular hypothalamus (PVH) (Figs. 4 and 10C–E). We identified a few Nts/FG+ neurons in the ARC and PVH of mice, though the number of ARC and PVH Nts afferents to the VTA are minor compared to the robust number of Nts afferents from the LHA (Fig. 4).

3.7. Midbrain and hindbrain

Examination of the dorsal midbrain revealed Nts/FG+ neurons in the inferior and dorsal portions of the superior colliculus (inSC and dSC) and anterior prectectal nucleus (APT) (Fig. 11B, C). The periaqueductal grey (PAG) contained many brainstem Nts afferents to the VTA that were evenly distributed throughout its rostrocaudal and dorsoventral extent, similar to the distribution shown in the lateral and ventrolateral (LPAG and VLPAG) sub-regions (Fig. 11D). While only 4–6 Nts/FG+ neurons were present in each coronal section of the PAG, they were consistently observed across the large rostrocaudal span of the PAG (approximately 2.5 mm); hence this continuum resulted in a substantial total number of Nts afferents to the VTA (Fig. 4) but modest density of PAG Nts afferents to the VTA compared to those arising from the LPO, MPO, LHA and NAsh (Table 2). We also detected small numbers of Nts/FG+ neurons in the PTg and LDTg (Fig. 11E, Fig. 12D).

Dense populations of GFP-labeled Nts neurons were noted in the parabrachial nucleus (PB) and the DR, but few of these contained FG, and thus provided minimal projections to the VTA (Fig. 12B, C). The lateral PB (LPB) contained segregated groups of either GFP or FG-labeled neurons with the GFP-labeled neurons clustered more laterally, and co-labeled neurons tended to be found in the middle where the two populations overlap (Fig. 12C). Nts neurons in the DR were most abundant in caudal sections between −4.8 to −5.0 bregma, which also gave rise to the highest numbers of colocalized neurons per section.

3.8. The VTA contains a small population of non-dopaminergic Nts neurons

Injection of FG into the VTA precluded assessment of local afferents, but to determine whether the VTA could serve as a local source of Nts input we examined the VTA of $Nts^{Cre};GFP$ mice for GFP expression. We observed very few Nts neurons within the boundaries of the VTA (372 ± 44 total neurons), which were predominantly localized in the caudolateral region (Fig. 13). 97% of these VTA Nts neurons did not colocalize with TH, indicating that most mouse VTA Nts neurons are not DA-ergic.

4. Discussion

Here, we characterized the endogenous sources of Nts that can directly regulate the VTA in mice. Our findings reveal that the largest source of mouse Nts input to the VTA comes from the hypothalamus, predominantly from the sub-regions of the LPO, MPO, and LHA. The NAsh also provides significant Nts afferents to the VTA, while the amygdala, VP, and sub-regions of the hindbrain provide more modest Nts input. To our knowledge this is the first comprehensive definition of mouse Nts afferents to the VTA, and is a first step toward understanding how Nts coordinates a diverse repertoire of behaviors in mice. Indeed, since Nts afferents from the MPO and LHA of mice modify DA-mediated social interaction and

energy balance, respectively (McHenry et al., 2017; Patterson et al., 2015; Woodworth et al., 2017b) it is possible that each Nts circuit orchestrates a specific motivated behavior via the VTA. Going forward it will be important to determine the particular roles of each Nts projection, and hence precise mechanisms to influence feeding, locomotor activity, social behavior, sleep, and response to addictive drugs.

4.1. Validation of the Nts^{Cre};GFP model and implications

Nts neurons have been previously difficult to identify because immunohistochemical reagents labeled fibers, but were insufficient to label cell bodies unless animals were pre-treated with lethal doses of the axonal transport inhibitor, colchicine (Leinninger et al., 2011). The requirement for colchicine treatment therefore limited study of Nts neurons and their contributions to normal physiology. Here we demonstrate that *Nts^{Cre};GFP* reporter mice faithfully identify colchicine-mediated Nts-IR cells, confirming the fidelity of these mice for identifying Nts, and their utility for future studies of the physiological contributions of Nts neurons. While most GFP-labeled cells in these mice co-localized with Nts-IR, we also observed a few GFP-labeled cells that did not. This could result from incomplete colchicine-mediated inhibition of axonal transport in all Nts neurons, or if colchincine-induced cell death occurs before there was sufficient Nts accumulation in the cell body to be detected via IR: both scenarios would prevent adequate detection via Nts-IR, but genetically-induced GFP labeling would be present. Another possible explanation is that the GFP-only cells expressed Nts at some point in development that permitted Cre-mediated recombination and GFP expression, but no longer actively express Nts in the adult state assessed here. Since Cre-mediated recombination induces permanent GFP expression, any developmentally-expressing Nts cells would remain GFP-labeled throughout the lifespan labeled despite their current Nts expression or lack thereof. However, few GFP-only cells were observed in the *Nts^{Cre};GFP* reporter mice, while essentially all of the Nts-IR cells were co-labeled with GFP, indicating that the model robustly and specifically identifies actively expressing Nts cells. Furthermore, an independent group recently analyzed the POA from the *Nts^{Cre};GFP* line via ISH and reported that 91% of the *Cre*-positive cells contained *Nts* but no *Nts*-positive cells were found without *Cre* (McHenry et al., 2017). These data are consistent with our results using colchicine-mediated Nts-IR in the *Nts^{Cre};GFP* line, and indicate that these mice can be used to correctly and quantitatively identify Nts neurons in the mouse brain.

Our data also revealed an important consideration when using the knock-in *Nts^{Cre};GFP* line: it identifies Nts cells, but does not reflect the amount of Nts peptide they express. Because the *Nts^{Cre};GFP* line includes an IRES-Cre cassette downstream of the Nts coding sequence, any Nts expression will lead to Cre expression, recombination and robust GFP expression. This many explain why we observed similarly bright GFP cells within the LHA, POA and NA, but variable levels of colchicine-mediated Nts-IR between these brain regions, and indeed between cells within the same brain region. The NA, for example, contains cells with weak Nts-IR compared to that of LHA and POA neurons, which is consistent with the intensity of *Nts* ISH across these regions (Fig. 1). Given that Nts-IR is low, but detectable, our data favor the interpretation that adult mouse NA Nts neurons express modest amounts of Nts message and peptide compared to hypothalamic Nts cells,

but are equivalently identified via GFP expression in the *Nts^{Cre};GFP* line (Fig. 1). Thus, the *Nts^{Cre};GFP* line faithfully identifies any Nts neuron, but the amount of induced-GFP cannot be used to differentiate cells expressing high vs. low levels of Nts peptide. The variable levels of Nts expression between cells within a region, coupled with the technical artifacts inherent to colchicine use (as detailed above), might explain our observation of some apparent "GFP-only" labeled cells. Indeed, cells expressing minimal amounts of Nts (such as those in the NA) may be unlikely to concentrate sufficient Nts peptide prior to their malfunction/death to permit immunodetection compared to hypothalamic cells expressing higher peptide levels. This type of technical artifact is avoided by directly assessing mRNA levels, and explains why an ISH study of the *Nts^{Cre}* line for *Nts* and *Cre* did not identify any "Cre-only" cells, despite clearly variable levels of Nts mRNA between cells (McHenry et al., 2017). Future studies using the *Nts^{Cre};GFP* line should be careful when interpreting the physiologic significance of the GFP-marked Nts cells, bearing in mind that the model does not quantitatively assess the amount of Nts peptide they express. This is an important consideration, since ISH and our colchicine-mediated Nts-IR data reveal significantly lower Nts expression in the NA compared to the LHA and POA regions of the hypothalamus. This might suggest that LHA and POA Nts neurons, in general, produce and release more Nts to their projection targets than NA Nts neurons, which could have functional implications for Nts-mediated signaling within the VTA. Going forward, stimulation of region-specific Nts afferents will be necessary to determine if their differential Nts expression causes distinct physiologic effects via the VTA.

Previously, immunohistochemistry was used to identify numerous Nts cell bodies in rats that co-express TH, and hence are DA-ergic (Bayer et al., 1991; Hokfelt et al., 1984; Studler et al., 1988), but very few Nts-expressing cells are detected in the mouse VTA via ISH (Lein et al., 2007). Using *Nts^{Cre};GFP* reporter mice we observed only a small population of GFP-labeled Nts neurons within the VTA, consistent with Nts ISH labeling in mice. Together these data illuminate important species disparities in Nts expression, and suggest that the Nts system may modify the VTA signaling via distinct mechanisms in mice and rats. For example, only 3% of mouse VTA Nts neurons co-expressed TH, thus the vast majority are not DA-ergic, in contrast to the largely DAergic VTA Nts cell bodies neurons described in rats (Hokfelt et al., 1984; Seroogy et al., 1988). Mouse VTA Nts neurons may instead contain either glutamate or GABA and project locally within the VTA to directly regulate DA neuron firing (Omelchenko and Sesack, 2009). Intriguingly, the small number of TH-negative Nts neurons was primarily detected in the caudal VTA along the rostral lateral borders, where the majority of VTA GABA neurons reside (Mazei-Robison and Nestler, 2012). These data suggest that mouse VTA Nts neurons could be GA-BAergic, and might provide local inhibitory control over neighboring DA neurons. Furthermore, our finding of few local VTA Nts neurons compared to the robust Nts input from the POA, LHA and NAsh suggests that external sources of Nts are the predominant mechanism to modulate the VTA and motivated behaviors. Thus, the use of *Nts^{Cre};GFP* mice reveals important functional differences in how Nts engages the VTA and perhaps DA signaling in mice and rats, which will be important to consider in future studies of Nts action in rodents.

4.2. Limitations of this study and potential impact on interpretations

The general retrograde tracer FG can be taken up by any terminals at the injection site, thus FG must be confined to the specific region of interest to accurately identify afferents (Schmued and Fallon, 1986). The cases analyzed herein were of mice with FG injections targeted to the VTA, spanning the medial to lateral subregions, but we cannot rule out the possibility of some FG spread into extra-VTA regions. Such spread could result in attribution of afferents to the VTA when they indeed arise from the minimal FG spread to VTA-adjacent regions. For example, FG spread to the midbrain reticular formation just above the VTA could result in the FG-labeled cells that we observed in the mouse ZI. Since the ZI projects to this midbrain reticular formation in rats, but not to the VTA (Zahm et al., 2011), it is possible that our current finding of ZI Nts projections to the VTA of mice results from such an experimental artifact (Zahm et al., 2011). This could account for the apparent ZI Nts afferents to VTA found in our mouse study, and the dearth of them previously reported from rats. However, two independent groups using Cre-specific retrograde tracing from Cre-containing VTA DA or GABA neurons determined that they receive direct projections from the ZI (Beier et al., 2015; Watabe-Uchida et al., 2012), supporting the possibility that some mouse ZI Nts neurons may indeed project specifically to the VTA. Another caveat of using FG is that the injections cause some unavoidable mechanical damage to the targeted tissue that impairs assessment of local circuits. As a result, we were unable to confidently assess any local VTA afferents arising from within the VTA itself or from the VTA-RMTg continuum, due to their close proximity to the FG injection site. However, given the paucity of Nts neurons in the VTA (Fig. 13), including the tail region that is thought to blend into the RMTg in mice (Bourdy and Barrot, 2012; Quina et al., 2015), it is unlikely that these local populations are a significant source of the Nts input to the VTA in mice. Additionally, FG can be taken up by damaged axons of passage near the injection site, which may lead to false-positive identification of afferents (Dado et al., 1990). Since it is nearly impossible to perfectly contain FG within the small mouse VTA, or prevent any damage to axons of passage, it is important to interpret our current findings with caution in light of these potential caveats. Lastly, since we did not use unbiased stereology in this investigation, we could not establish the absolute number of Nts afferents to the VTA. However, our objective was simply to compare the relative number and density of VTA afferents between Nts-containing brain sites, in order to guide future physiologic studies of Nts-mediated regulation of the VTA. Thus, our data from Fig. 4 and Table 2 should be interpreted as a comparative description of Nts afferents to the VTA. Despite these methodological provisos, our work does, at the least, narrow the potential sites of Nts inputs to the mouse VTA, which can be confirmed via future studies using Nts^{Cre} mice and genetically-and-location specified tract tracers.

4.3. Comparison to previous work

The VTA receives input from many brain structures (Faget et al., 2016; Geisler and Zahm, 2005; Phillipson, 1979; Watabe-Uchida et al., 2012), but we found that the mouse Nts afferents were confined to a limited number of regions. This result is not due to the $Nts^{Cre};GFP$ model under-reporting Nts neurons since essentially all Nts-IR neurons are identified by GFP and ISH confirms similar labeling fidelity in the line (McHenry et al., 2017). Instead, our data indicate that Nts input to the mouse VTA comes from relatively

circumscribed regions. For example, the DR, VP, and PBN provide major input to the VTA (Faget et al., 2016; Yetnikoff et al., 2015), and we also observed many FG-labeled neurons in these regions but very few were Nts-specific VTA afferents. The highest number of Nts-labeled VTA afferents in mice came from the POA, originating specifically from the MPO and LPO sub-regions. Intriguingly, the POA only provides ~2% of all VTA input in mouse (Faget et al., 2016), suggesting that the Nts projections likely comprise the majority of POA inputs to the VTA. Other significant sources of mouse Nts input to the VTA originated from the LHA and NAsh, regions that are essential for mediating ingestive and social reward behavior (Caggiula and Hoebel, 1966; Garris et al., 1999; Hoebel and Teitelbaum, 1962). Intriguingly, in mice, POA Nts neurons regulate social reward via the VTA (McHenry et al., 2017), while LHA Nts neurons modify locomotor activity and energy balance via the VTA (Patterson et al., 2015; Opland et al., 2013; Leinninger et al., 2011). Our current tracing results are thus consistent with these previously characterized Nts afferents to the VTA, and taken together this work suggests that region-specific sources of Nts input to the VTA may control distinct motivated behaviors. Overall our data support Geisler and Zahm's hypothesis that Nts inputs to the VTA preferentially originate from regions associated with mediating reward behaviors rather than aversion (Geisler and Zahm, 2006a).

We did note several discrepancies in the distribution of Nts afferents in mice compared to those in rats, indicative of species differences in Nts signaling. For example, rats have a continuous band of Nts afferents from the LPO and rostral LHA, while mice exhibit significant clusters of Nts afferents in the perifornical LHA (between −1.30 and −1.80 from bregma) and the LPO, with sparse afferents between these regions. Additionally, although mice and rats have many Nts neurons in the LS and endopiriform areas (Alexander et al., 1989; Sato et al., 1991), mice lack the substantial Nts-afferents from these regions to the VTA that were observed in rats. This discrepancy may be explained by the general paucity of VTA projections from the LS and endopiriform areas in mice (0.1–0.3% of all VTA afferents) compared to rats (~2–3% of all VTA afferents) (Faget et al., 2016; Yetnikoff et al., 2015). Mice also appear to lack the significant Nts projections from the DR and LS to the VTA that have been described in rats (Geisler and Zahm, 2006a). In contrast, mice have more Nts afferents to the VTA originating from the ZI and the NAsh. Indeed, the mouse ZI and LHA contain comparable total numbers of Nts neurons projecting to the VTA (Fig. 4), but more sparse ZI Nts projections to the VTA were observed in rats (Zahm et al., 2011). Intriguingly, a higher density of mouse Nts inputs to the VTA arise from the LHA compared to the ZI, despite equivalent total numbers of afferents observed in each site (Table 2 and Fig. 4); the concentration of LHA Nts afferents may suggest a more important physiologic role for this population in regulating the VTA than the sparse ZI projections. Furthermore, our mouse data are consistent with reports of rat Nts afferents to the VTA from the NAsh, BNST and amygdala, but the density of afferents differs between species. For example, Geisler and Zahm reported a minor NAsh Nts input to the VTA in rats (Geisler and Zahm, 2006a), but our analysis in mice identifies the NAsh as one of the most significant contributors of total Nts neurons providing input to the VTA (Fig. 4). Since these Nts/FG+ cells were distributed across the large expanse of the NAsh, they provided less dense projections to the VTA than other regions with comparable total numbers of Nts/FG+ cells, such as the LPO and MPO (Table 2). Along with the sparse distribution of NAsh

Nts afferents to VTA, these NA neurons express minimal amounts of Nts peptide, which raises questions about whether NA-released Nts mediates significant physiologic effects vs. the robust amounts of Nts that is released from hypothalamic afferents to the VTA. Going forward it will be important to test the role of Nts from the NA vs. hypothalamus to determine if these afferents mediate differential effects and/or act upon different VTA targets. We also detected small populations of VTA-projecting Nts neurons in the APT, PAG, and SC, which were not previously identified in rats. Overall, our data suggest species-conserved Nts circuits from the LHA and POA that can engage the VTA, but also point to other species-specific mechanisms for Nts action that may have functional importance. While we cannot rule out that the apparent differences between mice and rats could be due to technical artifacts (e.g. differences in retrograde tracer spread), the fact that mice and rats have vastly different VTA Nts expression (Fig. 13) at least suggests some species differences in central Nts signaling, and warrants further careful assessment of both rodent models.

4.4. Functional implications for Nts afferents to the VTA

It is now recognized that the VTA contains functionally-distinct populations of neurons that differentially regulate reward, aversion or fear behaviors (Cohen et al., 2012; Faure et al., 2008; Lammel et al., 2012; Tan et al., 2012; van Zessen et al., 2012). Mapping the VTA inputs that target specific subpopulations of VTA neurons may therefore point the way to directing certain behaviors, and could have far-reaching impact on treatment of many psychiatric conditions. Nts is one signal that can act within the VTA, largely indicated via pharmacological studies; yet, there has remained a gap in the field concerning which populations of Nts neurons provide endogenous Nts to the VTA, and if/how they engage specific VTA neurons to modify behavior. Our findings reveal multiple populations of Nts neurons throughout the mouse brain that project to the VTA. However, given the abundance of Nts-expressing populations projecting to the VTA, their variability in Nts peptide expression levels, and data suggesting that distinct Nts populations mediate different behaviors, it is likely that the Nts populations described here engage and act via different populations of VTA neurons. For example, stimulation of medial POA Nts neurons that project to the VTA promotes social reward that is influenced by estradiol levels, suggesting that this circuit may contribute to sexual receptivity and/or reward behavior (McHenry et al., 2017). These POA Nts neurons did not, however, modulate rewarding feeding behavior. By contrast, experimental activation of LHA Nts neurons, at least some of which project to the VTA, suppressed motivated feeding while promoting drinking and locomotor activity, which led to weight loss (Woodworth et al., 2017b). LHA Nts-mediated feeding suppression and DA release to the NA was dependent on signaling via Nts receptor-1, thus, Nts released from LHA Nts neurons likely acts directly via the subset of VTA neurons that co-express Nts receptor-1 and DA (Woodworth et al., 2017a, b). It has yet to be determined whether POA Nts neurons that project to the VTA mediate behavior via release of Nts and regulation of Nts receptor-1 expressing DA neurons or via the many Nts receptor-2 expressing glia in this region (Woodworth et al., 2017a). Since many POA and LHA neurons produce high levels of Nts, however, it is likely that these populations exert at least some of their actions via Nts signaling. Given that such different behaviors were regulated by the POA Nts vs. LHA Nts neurons, it seems likely that their released signals are mediated via different subsets of VTA neurons, and possibly via a different Nts receptor isoform. Based on these data, it is

tempting to speculate that Nts afferents from other regions might engage specific VTA cells to mediate other behaviors ascribed to Nts, such as analgesia or to attenuate the reinforcing effects of drugs of abuse (Schroeder and Leinninger, 2017).

Our findings confirm that there are several large populations of VTA-projecting Nts neurons distributed throughout the brain of mice, and raises the possibility that they may be functionally and neurochemically distinct from each other. For example, only the Nts neurons in the LHA are regulated by the anorectic hormone leptin (Leinninger et al., 2011), while POA Nts neurons are specifically regulated by sex-specific odor cues and sex steroids (McHenry et al., 2017). It is therefore tempting to speculate that different populations of Nts neurons receive specific physiologic cues, and in response, release their unique set of transmitters to regulate the VTA and output behavior. While we have focused on defining Nts-expressing afferents to the VTA, it is likely that these neurons also express other transmitters, whose release might produce differential effects in the VTA. For example, at least some LHA Nts neurons co-express the neuropeptide galanin, though they appear to predominantly project within the LHA and not to the VTA (Laque et al., 2015; Qualls-Creekmore et al., 2017). Different populations of Nts neurons might vary in classical neurotransmitter content, and hence release of Nts along with inhibitory GABA or excitatory glutamate could lead to very different effects within the VTA. Nts afferents to the VTA may also be differentially regulated in males and females. In addition to the estradiol-mediated and sex-specific regulation of POA Nts afferents to the VTA (McHenry et al., 2017), altered Nts signaling has been linked to anorexia nervosa, a disorder predominantly diagnosed in females. Thus, there are likely gene × sex interactions to be characterized within the Nts signaling system that coordinate energy balance (Lutter et al., 2017), though it is yet to be determined if these are mediated via the POA and or afferents to the VTA. By identifying the specific populations of Nts neurons that provide input to the VTA, our work paves the way for subsequent neurochemical phenotyping, which is essential to determine how these populations engage the VTA to mediate behavior.

5. Conclusions

Collectively, our work defines the central circuits capable of providing endogenous Nts to the VTA in mice, which are summarized in Figs. 3–4 and Table 2. These data will be useful to direct the application of optogenetic and/or chemogenetic strategies to selectively modulate the activity of site-specified Nts populations, and thereby to define their contributions to behavior and physiology. One limitation of our present work is that it identifies Nts neurons that project to the VTA in general, but does not reveal which specific VTA neurons are targets of Nts signaling (e.g. DAergic, GABAergic, and/or glutamatergic neurons). Since it is now appreciated that VTA neuronal subpopulations control specific motivated behaviors and their reinforcing or aversive valence, it will be crucial to establish how Nts neurons mechanistically engage VTA neurons to fully understand their role in behavior. Indeed, given that Nts inputs from the LHA and POA appear to differentially modify motivated behaviors, there may be distributed Nts circuits and Nts mechanisms to appropriately coordinate environmental stimuli with feeding, arousal and/or social interaction responses. Modulation of specific Nts afferents to the VTA may therefore be useful to normalize maladaptive behaviors and to improve health.

Acknowledgments

We thank David P. Olson (University of Michigan) for graciously sharing the Cre-inducible Rosa$^{eGFP\text{-}L10a}$ reporter line used in these studies. This research was supported by the grants from the NIH to HLW (F30-DK107163), JAB (F31-DK107081) and GML (R01-DK103808).

References

Alexander MJ, Miller MA, Dorsa DM, Bullock BP, Melloni RH Jr, Dobner PR, Leeman SE. 1989; Distribution of neurotensin/neuromedin N mRNA in rat fore-brain: unexpected abundance in hippocampus and subiculum. Proc Natl Acad Sci U S A. 86 :5202–5206. [PubMed: 2740352]

Bayer VE, Towle AC, Pickel VM. 1991; Vesicular and cytoplasmic localization of neurotensin-like immunoreactivity (NTLI) in neurons postsynaptic to terminals containing NTLI and/or tyrosine hydroxylase in the rat central nucleus of the amygdala. J Neurosci Res. 30 :398–413. [PubMed: 1686786]

Beaudet A, Woulfe J. 1992; Morphological substrate for neurotensin-dopamine interactions in the rat midbrain tegmentum. Ann N Y Acad Sci. 668 :173–185. [PubMed: 1361112]

Beck B, Burlet A, Nicolas JP, Burlet C. 1989; Neurotensin in microdissected brain nuclei and in the pituitary of the lean and obese Zucker rats. Neuropeptides. 13 :1–7. [PubMed: 2922104]

Beier KT, Steinberg EE, DeLoach KE, Xie S, Miyamichi K, Schwarz L, Gao XJ, Kremer EJ, Malenka RC, Luo L. 2015; Circuit architecture of VTA dopamine neurons revealed by systematic input-output mapping. Cell. 162 (3) :622–634. [PubMed: 26232228]

Boules M, Oliveros A, Liang Y, Williams K, Shaw A, Robinson J, Fredrickson P, Richelson E. 2011; A neurotensin analog, NT69L, attenuates intravenous nicotine self-administration in rats. Neuropeptides. 45 :9–16. [PubMed: 21047685]

Boules MM, Fredrickson P, Muehlmann AM, Richelson E. 2014; Elucidating the role of neurotensin in the pathophysiology and management of major mental disorders. Behav Sci (Basel, Switzerland). 4 :125–153.

Bourdy R, Barrot M. 2012; A new control center for dopaminergic systems: pulling the VTA by the tail. Trends Neurosci. 35 :681–690. [PubMed: 22824232]

Bromberg-Martin ES, Matsumoto M, Hikosaka O. 2010; Dopamine in motivational control: rewarding, aversive, and alerting. Neuron. 68 :815–834. [PubMed: 21144997]

Brown JA, Bugescu R, Mayer TA, Gata-Garcia A, Kurt G, Woodworth HL, Leinninger GM. 2017; Loss of action via Neurotensin-leptin receptor neurons disrupts leptin and ghrelin-mediated control of energy balance. Endocrinology. 158 :1271–1288. [PubMed: 28323938]

Caceda R, Binder EB, Kinkead B, Nemeroff CB. 2012; The role of endogenous neurotensin in psychostimulant-induced disruption of prepulse inhibition and locomotion. Schizophr Res. 136 :88–95. [PubMed: 22104138]

Cador M, Kelley AE, Le Moal M, Stinus L. 1986; Ventral tegmental area infusion of substance P, neurotensin and enkephalin: differential effects on feeding behavior. Neuroscience. 18 :659–669. [PubMed: 2427971]

Caggiula AR, Hoebel BG. 1966; “Copulation-reward site” in the posterior hypothalamus. Science (New York, NY). 153 :1284–1285.

Cape EG, Manns ID, Alonso A, Beaudet A, Jones BE. 2000; Neurotensin-induced bursting of cholinergic basal forebrain neurons promotes gamma and theta cortical activity together with waking and paradoxical sleep. J Neurosci. 20 :8452–8461. [PubMed: 11069953]

Carey LM, Rice RJ, Prus AJ. 2017; The Neurotensin NTS1 receptor agonist PD149163 produces antidepressant-like effects in the forced swim test: further support for neurotensin as a novel pharmacologic strategy for antidepressant drugs. Drug Dev Res. 78 :196–202. [PubMed: 28736839]

Carr DB, Sesack SR. 2000; GABA-containing neurons in the rat ventral tegmental area project to the prefrontal cortex. Synapse (New York, NY). 38 :114–123.

Carraway R, Leeman SE. 1973; The isolation of a new hypotensive peptide, neuro-tensin, from bovine hypothalami. J Biol Chem. 248 :6854–6861. [PubMed: 4745447]

Carraway R, Leeman SE. 1976; Characterization of radioimmunoassayable neuro-tensin in the rat. Its differential distribution in the central nervous system, small intestine, and stomach. J Biol Chem. 251 :7045–7052. [PubMed: 993203]

Cohen JY, Haesler S, Vong L, Lowell BB, Uchida N. 2012; Neuron-type-specific signals for reward and punishment in the ventral tegmental area. Nature. 482 :85–88. [PubMed: 22258508]

Cooke JH, Patterson M, Patel SR, Smith KL, Ghatei MA, Bloom SR, Murphy KG. 2009; Peripheral and central administration of xenin and neurotensin suppress food intake in rodents. Obesity (Silver Spring, Md). 17 :1135–1143.

Dado RJ, Burstein R, Cliffer KD, Giesler GJ Jr. 1990; Evidence that Fluoro-Gold can be transported avidly through fibers of passage. Brain Res. 533 :329–333. [PubMed: 1705157]

Demeule M, Beaudet N, Regina A, Besserer-Offroy E, Murza A, Tetreault P, Belleville K, Che C, Larocque A, Thiot C, Beliveau R, Longpre JM, Marsault E, Leduc R, Lachowicz JE, Gonias SL, Castaigne JP, Sarret P. 2014; Conjugation of a brain-penetrant peptide with neurotensin provides antinociceptive properties. J Clin Invest. 124 :1199–1213. [PubMed: 24531547]

Ellenbroek BA, Angelucci F, Husum H, Mathe AA. 2016; Gene-environment interactions in a rat model of depression. Maternal separation affects neurotensin in selected brain regions. Neuropeptides. 59 :83–88. [PubMed: 27372546]

Elliott PJ, Nemeroff CB. 1986; Repeated neurotensin administration in the ventral tegmental area: effects on baseline and D-amphetamine-induced locomotor activity. Neurosci Lett. 68 :239–244. [PubMed: 3748452]

Elliott PJ, Chan J, Parker YM, Nemeroff CB. 1986; Behavioral effects of neuro-tensin in the open field: structure-activity studies. Brain Res. 381 :259–265. [PubMed: 3756503]

Ervin GN, Birkemo LS, Nemeroff CB, Prange AJ Jr. 1981; Neurotensin blocks certain amphetamine-induced behaviours. Nature. 291 :73–76. [PubMed: 7231526]

Faget L, Osakada F, Duan J, Ressler R, Johnson AB, Proudfoot JA, Yoo JH, Callaway EM, Hnasko TS. 2016; Afferent inputs to neurotransmitter-defined cell types in the ventral tegmental area. Cell Rep. 15 :2796–2808. [PubMed: 27292633]

Faure A, Reynolds SM, Richard JM, Berridge KC. 2008; Mesolimbic dopamine in desire and dread: enabling motivation to be generated by localized glutamate disruptions in nucleus accumbens. J Neurosci. 28 :7184–7192. [PubMed: 18614688]

Feifel D, Reza TL. 1999; Effects of neurotensin administered into the ventral tegmental area on prepulse inhibition of startle. Behav Brain Res. 106 :189–193. [PubMed: 10595435]

Ferraro L, Tiozzo Fasiolo L, Beggiato S, Borelli AC, Pomierny-Chamiolo L, Frankowska M, Antonelli T, Tomasini MC, Fuxe K, Filip M. 2016; Neurotensin: a role in substance use disorder? J Psychopharmacol (Oxford, England). 30 :112–127.

Fitzpatrick K, Winrow CJ, Gotter AL, Millstein J, Arbuzova J, Brunner J, Kasarskis A, Vitaterna MH, Renger JJ, Turek FW. 2012; Altered sleep and affect in the neurotensin receptor 1 knockout mouse. Sleep. 35 :949–956. [PubMed: 22754041]

Gammie SC, D'Anna KL, Gerstein H, Stevenson SA. 2009; Neurotensin inversely modulates maternal aggression. Neuroscience. 158 :1215–1223. [PubMed: 19118604]

Garris PA, Kilpatrick M, Bunin MA, Michael D, Walker QD, Wightman RM. 1999; Dissociation of dopamine release in the nucleus accumbens from intracranial self-stimulation. Nature. 398 :67–69. [PubMed: 10078530]

Geisler S, Zahm DS. 2005; Afferents of the ventral tegmental area in the rat-anatomical substratum for integrative functions. J Comp Neurol. 490 :270–294. [PubMed: 16082674]

Geisler S, Zahm DS. 2006a; Neurotensin afferents of the ventral tegmental area in the rat: [1] re-examination of their origins and [2] responses to acute psychostimulant and antipsychotic drug administration. Eur J Neurosci. 24 :116–134. [PubMed: 16882012]

Geisler S, Zahm DS. 2006b; On the retention of neurotensin in the ventral tegmental area (VTA) despite destruction of the main neurotensinergic afferents of the VTA—implications for the organization of forebrain projections to the VTA. Brain Res. 1087 :87–104. [PubMed: 16626637]

Glimcher PW, Margolin DH, Giovino AA, Hoebel BG. 1984; Neurotensin: a new 'reward peptide'. Brain Res. 291 :119–124. [PubMed: 6320951]

Glimcher PW, Giovino AA, Hoebel BG. 1987; Neurotensin self-injection in the ventral tegmental area. Brain Res. 403 :147–150. [PubMed: 3828807]

Hoebel BG, Teitelbaum P. 1962; Hypothalamic control of feeding and self-stimulation. Science (New York, NY). 135 :375–377.

Hokfelt T, Everitt BJ, Theodorsson-Norheim E, Goldstein M. 1984; Occurrence of neurotensinlike immunoreactivity in subpopulations of hypothalamic, mesencephalic, and medullary catecholamine neurons. J Comp Neurol. 222 :543–559. [PubMed: 6365985]

Howes OD, McCutcheon R, Owen MJ, Murray RM. 2017; The role of genes, stress, and dopamine in the development of schizophrenia. Biol Psychiatry. 81 :9–20. [PubMed: 27720198]

Jennes L, Stumpf WE, Kalivas PW. 1982; Neurotensin: topographical distribution in rat brain by immunohistochemistry. J Comp Neurol. 210 :211–224. [PubMed: 6754769]

Jolicoeur FB, Rivest R, St-Pierre S, Gagne MA, Dumais M. 1985; The effects of neurotensin and [D-Tyr11]-NT on the hyperactivity induced by intra-accumbens administration of a potent dopamine receptor agonist. Neuropeptides. 6 :143–156. [PubMed: 2987745]

Kalivas PW, Duffy P. 1990; Effect of acute and daily neurotensin and enkephalin treatments on extracellular dopamine in the nucleus accumbens. J Neurosci. 10 :2940–2949. [PubMed: 1697899]

Kalivas PW, Taylor S. 1985; Behavioral and neurochemical effect of daily injection with neurotensin into the ventral tegmental area. Brain Res. 358 :70–76. [PubMed: 4075132]

Kalivas PW, Nemeroff CB, Prange AJ Jr. 1981; Increase in spontaneous motor activity following infusion of neurotensin into the ventral tegmental area. Brain Res. 229 :525–529. [PubMed: 7306825]

Kalivas PW, Burgess SK, Nemeroff CB, Prange AJ Jr. 1983; Behavioral and neurochemical effects of neurotensin microinjection into the ventral tegmental area of the rat. Neuroscience. 8 :495–505. [PubMed: 6406930]

Kalivas PW, Nemeroff CB, Prange AJ Jr. 1984; Neurotensin microinjection into the nucleus accumbens antagonizes dopamine-induced increase in locomotion and rearing. Neuroscience. 11 :919–930. [PubMed: 6738859]

Keith, BJ, Franklin, GP. The Mouse Brain in Stereotaxic Coordinates. Third. Elsevier; 2007.

Kelley AE, Cador M, Stinus L, Le Moal M. 1989; Neurotensin, substance P, neurokinin-alpha, and enkephalin: injection into ventral tegmental area in the rat produces differential effects on operant responding. Psychopharmacology. 97 :243–252. [PubMed: 2471221]

Kempadoo KA, Tourino C, Cho SL, Magnani F, Leinninger GM, Stuber GD, Zhang F, Myers MG, Deisseroth K, de Lecea L, Bonci A. 2013; Hypothalamic neurotensin projections promote reward by enhancing glutamate transmission in the VTA. J Neurosci. 33 :7618–7626. [PubMed: 23637156]

Kim ER, Mizuno TM. 2010; Role of neurotensin receptor 1 in the regulation of food intake by neuromedins and neuromedin-related peptides. Neurosci Lett. 468 :64–67. [PubMed: 19857548]

Kitabgi P, De Nadai F, Cuber JC, Dubuc I, Nouel D, Costentin J. 1990; Calcium-dependent release of neuromedin N and neurotensin from mouse hypothalamus. Neuropeptides. 15 :111–114. [PubMed: 2080018]

Krashes MJ, Shah BP, Madara JC, Olson DP, Strochlic DE, Garfield AS, Vong L, Pei H, Watabe-Uchida M, Uchida N, Liberles SD, Lowell BB. 2014; An excitatory paraventricular nucleus to AgRP neuron circuit that drives hunger. Nature. 507 :238–242. [PubMed: 24487620]

Lammel S, Lim BK, Ran C, Huang KW, Betley MJ, Tye KM, Deisseroth K, Malenka RC. 2012; Input-specific control of reward and aversion in the ventral tegmental area. Nature. 491 :212–217. [PubMed: 23064228]

Laque A, Yu S, Qualls-Creekmore E, Gettys S, Schwartzenburg C, Bui K, Rhodes C, Berthoud HR, Morrison CD, Richards BK, Munzberg H. 2015; Leptin modulates nutrient reward via inhibitory galanin action on orexin neurons. Mol Metab. 4 :706–717. [PubMed: 26500842]

Legault M, Congar P, Michel FJ, Trudeau LE. 2002; Presynaptic action of neuro-tensin on cultured ventral tegmental area dopaminergic neurones. Neuroscience. 111 :177–187. [PubMed: 11955721]

Lein ES, Hawrylycz MJ, Ao N, Ayres M, Bensinger A, Bernard A, Boe AF, Boguski MS, Brockway KS, Byrnes EJ, Chen L, Chen L, Chen TM, Chin MC, Chong J, Crook BE, Czaplinska A, Dang CN, Datta S, Dee NR, Desaki AL, Desta T, Diep E, Dolbeare TA, Donelan MJ, Dong HW,

Dougherty JG, Duncan BJ, Ebbert AJ, Eichele G, Estin LK, Faber C, Facer BA, Fields R, Fischer SR, Fliss TP, Frensley C, Gates SN, Glattfelder KJ, Halverson KR, Hart MR, Hohmann JG, Howell MP, Jeung DP, Johnson RA, Karr PT, Kawal R, Kidney JM, Knapik RH, Kuan CL, Lake JH, Laramee AR, Larsen KD, Lau C, Lemon TA, Liang AJ, Liu Y, Luong LT, Michaels J, Morgan JJ, Morgan RJ, Mortrud MT, Mosqueda NF, Ng LL, Ng R, Orta GJ, Overly CC, Pak TH, Parry SE, Pathak SD, Pearson OC, Puchalski RB, Riley ZL, Rockett HR, Rowland SA, Royall JJ, Ruiz MJ, Sarno NR, Schaffnit K, Shapovalova NV, Sivisay T, Slaughterbeck CR, Smith SC, Smith KA, Smith BI, Sodt AJ, Stewart NN, Stumpf KR, Sunkin SM, Sutram M, Tam A, Teemer CD, Thaller C, Thompson CL, Varnam LR, Visel A, Whitlock RM, Wohnoutka PE, Wolkey CK, Wong VY, Wood M, Yaylaoglu MB, Young RC, Youngstrom BL, Yuan XF, Zhang B, Zwingman TA, Jones AR. 2007; Genome-wide atlas of gene expression in the adult mouse brain. Nature. 445 :168–176. [PubMed: 17151600]

Leinninger GM, Opland DM, Jo YH, Faouzi M, Christensen L, Cappellucci LA, Rhodes CJ, Gnegy ME, Becker JB, Pothos EN, Seasholtz AF, Thompson RC, Myers MG Jr. 2011; Leptin action via neurotensin neurons controls orexin, the mesolimbic dopamine system and energy balance. Cell Metab. 14 :313–323. [PubMed: 21907138]

Li J, Song J, Zaytseva YY, Liu Y, Rychahou P, Jiang K, Starr ME, Kim JT, Harris JW, Yiannikouris FB, Katz WS, Nilsson PM, Orho-Melander M, Chen J, Zhu H, Fahrenholz T, Higashi RM, Gao T, Morris AJ, Cassis LA, Fan TW, Weiss HL, Dobner PR, Melander O, Jia J, Evers BM. 2016; An obligatory role for neurotensin in high-fat-diet-induced obesity. Nature. 533 :411–415. [PubMed: 27193687]

Lutter M, Bahl E, Hannah C, Hofammann D, Acevedo S, Cui H, McAdams CJ, Michaelson JJ. 2017; Novel and ultra-rare damaging variants in neuropeptide signaling are associated with disordered eating behaviors. PLoS One. 12 :e0181556. [PubMed: 28846695]

Luttinger D, King RA, Sheppard D, Strupp J, Nemeroff CB, Prange AJ Jr. 1982; The effect of neurotensin on food consumption in the rat. Eur J Pharmacol. 81 :499–503. [PubMed: 6811292]

Margolis EB, Toy B, Himmels P, Morales M, Fields HL. 2012; Identification of rat ventral tegmental area GABAergic neurons. PLoS One. 7 :e42365. [PubMed: 22860119]

Mazei-Robison MS, Nestler EJ. 2012; Opiate-induced molecular and cellular plasticity of ventral tegmental area and locus coeruleus catecholamine neurons. Cold Spring Harbor Perspect Med. 2 :a012070.

McHenry JA, Otis JM, Rossi MA, Robinson JE, Kosyk O, Miller NW, McElligott ZA, Budygin EA, Rubinow DR, Stuber GD. 2017; Hormonal gain control of a medial preoptic area social reward circuit. Nat Neurosci. 20 :449–458. [PubMed: 28135243]

Meisenberg G, Simmons WH. 1985; Motor hypoactivity induced by neurotensin and related peptides in mice. Pharmacol Biochem Behav. 22 :189–193. [PubMed: 3983212]

Merullo DP, Cordes MA, Stevenson SA, Riters LV. 2015a; Neurotensin immunolabeling relates to sexually-motivated song and other social behaviors in male European starlings (Sturnus Vulgaris). Behav Brain Res. 282 :133–143. [PubMed: 25595421]

Merullo DP, Cordes MA, Susan DeVries M, Stevenson SA, Riters LV. 2015b; Neurotensin neural mRNA expression correlates with vocal communication and other highly-motivated social behaviors in male European starlings. Physiol Behav. 151 :155–161. [PubMed: 26192712]

Nemeroff CB, Luttinger D, Hernandez DE, Mailman RB, Mason GA, Davis SD, Widerlov E, Frye GD, Kilts CA, Beaumont K, Breese GR, Prange AJ Jr. 1983; Interactions of neurotensin with brain dopamine systems: biochemical and behavioral studies. J Pharmacol Exp Ther. 225 :337–345. [PubMed: 6682440]

Nestler EJ, Carlezon WA Jr. 2006; The mesolimbic dopamine reward circuit in depression. Biol Psychiatry. 59 :1151–1159. [PubMed: 16566899]

Omelchenko N, Sesack SR. 2009; Ultrastructural analysis of local collaterals of rat ventral tegmental area neurons: GABA phenotype and synapses onto dopamine and GABA cells. Synapse (New York, NY). 63 :895–906.

Opland D, Sutton A, Woodworth H, Brown J, Bugescu R, Garcia A, Christensen L, Rhodes C, Myers M Jr, Leinninger G. 2013; Loss of neurotensin receptor-1 disrupts the control of the mesolimbic dopamine system by leptin and promotes hedonic feeding and obesity. Mol Metab. 2 :423–434. [PubMed: 24327958]

Panayi F, Colussi-Mas J, Lambas-Senas L, Renaud B, Scarna H, Berod A. 2005; Endogenous neurotensin in the ventral tegmental area contributes to amphetamine behavioral sensitization. Neuropsychopharmacology. 30 :871–879. [PubMed: 15637639]

Patterson CM, Wong JM, Leinninger GM, Allison MB, Mabrouk OS, Kasper CL, Gonzalez IE, Mackenzie A, Jones JC, Kennedy RT, Myers MG Jr. 2015; Ventral tegmental area neurotensin signaling links the lateral hypothalamus to locomotor activity and striatal dopamine efflux in male mice. Endocrinology. 156 :1692–1700. [PubMed: 25734363]

Phillipson OT. 1979; Afferent projections to the ventral tegmental area of Tsai and interfascicular nucleus: a horseradish peroxidase study in the rat. J Comp Neurol. 187 :117–143. [PubMed: 489776]

Qualls-Creekmore E, Yu S, Francois M, Hoang J, Huesing C, Bruce-Keller A, Burk D, Berthoud HR, Morrison CD, Munzberg H. 2017; Galanin-expressing GABA neurons in the lateral hypothalamus modulate food reward and noncompulsive locomotion. J Neurosci. 37 :6053–6065. [PubMed: 28539422]

Quina LA, Tempest L, Ng L, Harris JA, Ferguson S, Jhou TC, Turner EE. 2015; Efferent pathways of the mouse lateral habenula. J Comp Neurol. 523 :32–60. [PubMed: 25099741]

Rompre PP, Gratton A. 1993; Mesencephalic microinjections of neurotensin-(1-13) and its C-terminal fragment, neurotensin-(8-13) potentiate brain stimulation reward. Brain Res. 616 :154–162. [PubMed: 8358607]

Rothwell PE. 2016; Autism spectrum disorders and drug addiction: common pathways, common molecules, distinct disorders? Front Neurosci. 10 :20. [PubMed: 26903789]

Rouibi K, Bose P, Rompre PP, Warren RA. 2015; Ventral midbrain NTS1 receptors mediate conditioned reward induced by the neurotensin analog, D-Tyr[11]neurotensin. Front Neurosci. 9 :470. [PubMed: 26733785]

Salamone JD, Correa M. 2012; The mysterious motivational functions of mesolimbic dopamine. Neuron. 76 :470–485. [PubMed: 23141060]

Sarhan S, Hitchcock JM, Grauffel CA, Wettstein JG. 1997; Comparative anti-psychotic profiles of neurotensin and a related systemically active peptide agonist. Peptides. 18 :1223–1227. [PubMed: 9396065]

Sato M, Kiyama H, Yoshida S, Saika T, Tohyama M. 1991; Postnatal ontogeny of cells expressing prepro-neurotensin/neuromedin N mRNA in the rat forebrain and midbrain: a hybridization histochemical study involving isotope-labeled and enzyme-labeled probes. J Comp Neurol. 310 :300–315. [PubMed: 1787175]

Schmued LC, Fallon JH. 1986; Fluoro-Gold: a new fluorescent retrograde axonal tracer with numerous unique properties. Brain Res. 377 :147–154. [PubMed: 2425899]

Schroeder LE, Leinninger GM. 2017; Role of central neurotensin in regulating feeding: implications for the development and treatment of body weight disorders. Biochim Biophys Acta. 1864 (1864) :900–916.

Seroogy K, Ceccatelli S, Schalling M, Hokfelt T, Frey P, Walsh J, Dockray G, Brown J, Buchan A, Goldstein M. 1988; A subpopulation of dopaminergic neurons in rat ventral mesencephalon contains both neurotensin and cholecystokinin. Brain Res. 455 :88–98. [PubMed: 3046712]

Seutin V, Massotte L, Dresse A. 1989; Electrophysiological effects of neurotensin on dopaminergic neurones of the ventral tegmental area of the rat in vitro. Neuropharmacology. 28 :949–954. [PubMed: 2572997]

Skoog KM, Cain ST, Nemeroff CB. 1986; Centrally administered neurotensin suppresses locomotor hyperactivity induced by d-amphetamine but not by scopolamine or caffeine. Neuropharmacology. 25 :777–782. [PubMed: 3748325]

Smith KE, Boules M, Williams K, Richelson E. 2012; NTS1 and NTS2 mediate analgesia following neurotensin analog treatment in a mouse model for visceral pain. Behav Brain Res. 232 :93–97. [PubMed: 22504145]

Smits SM, Terwisscha van Scheltinga AF, van der Linden AJ, Burbach JP, Smidt MP. 2004; Species differences in brain pre-pro-neurotensin/neuromedin N mRNA distribution: the expression pattern in mice resembles more closely that of primates than rats. Brain Res Mol Brain Res. 125 :22–28. [PubMed: 15193419]

Sotty F, Souliere F, Brun P, Chouvet G, Steinberg R, Soubrie P, Renaud B, Suaud-Chagny MF. 1998; Differential effects of neurotensin on dopamine release in the caudal and rostral nucleus accumbens: a combined in vivo electrochemical and electrophysiological study. Neuroscience. 85 :1173–1182. [PubMed: 9681955]

Sotty F, Brun P, Leonetti M, Steinberg R, Soubrie P, Renaud B, Suaud-Chagny MF. 2000; Comparative effects of neurotensin, neurotensin(8–13) and [D-Tyr(11)] neurotensin applied into the ventral tegmental area on extracellular dopamine in the rat prefrontal cortex and nucleus accumbens. Neuroscience. 98 :485–492. [PubMed: 10869842]

Stamatakis AM, Jennings JH, Ung RL, Blair GA, Weinberg RJ, Neve RL, Boyce F, Mattis J, Ramakrishnan C, Deisseroth K, Stuber GD. 2013; A unique population of ventral tegmental area neurons inhibits the lateral habenula to promote reward. Neuron. 80 :1039–1053. [PubMed: 24267654]

Steinberg R, Brun P, Fournier M, Souilhac J, Rodier D, Mons G, Terranova JP, Le Fur G, Soubrie P. 1994; SR 48692, a non-peptide neurotensin receptor antagonist differentially affects neurotensin-induced behaviour and changes in dopaminergic transmission. Neuroscience. 59 :921–929. [PubMed: 8058127]

Steinberg R, Brun P, Souilhac J, Bougault I, Leyris R, Le Fur G, Soubrie P. 1995; Neurochemical and behavioural effects of neurotensin vs [D-Tyr11] neurotensin on mesolimbic dopaminergic function. Neuropeptides. 28 :43–50. [PubMed: 7746351]

St-Gelais F, Legault M, Bourque MJ, Rompre PP, Trudeau LE. 2004; Role of calcium in neurotensin-evoked enhancement in firing in mesencephalic dopamine neurons. J Neurosci. 24 :2566–2574. [PubMed: 15014132]

Studler JM, Kitabgi P, Tramu G, Herve D, Glowinski J, Tassin JP. 1988; Extensive co-localization of neurotensin with dopamine in rat meso-cortico-frontal dopaminergic neurons. Neuropeptides. 11 :95–100. [PubMed: 3133572]

Szigethy E, Beaudet A. 1989; Correspondence between high affinity 125I-neurotensin binding sites and dopaminergic neurons in the rat substantia nigra and ventral tegmental area: a combined radioautographic and immunohistochemical light microscopic study. J Comp Neurol. 279 :128–137. [PubMed: 2563267]

Tan KR, Yvon C, Turiault M, Mirzabekov JJ, Doehner J, Labouebe G, Deisseroth K, Tye KM, Luscher C. 2012; GABA neurons of the VTA drive conditioned place aversion. Neuron. 73 :1173–1183. [PubMed: 22445344]

Theoharides TC, Tsilioni I, Patel AB, Doyle R. 2016; Atopic diseases and inflammation of the brain in the pathogenesis of autism spectrum disorders. Transl Psychiatry. 6 :e844. [PubMed: 27351598]

Uhl GR, Goodman RR, Snyder SH. 1979; Neurotensin-containing cell bodies, fibers and nerve terminals in the brain stem of the rat: immunohistochemical mapping. Brain Res. 167 :77–91. [PubMed: 378326]

Vadnie CA, Hinton DJ, Choi S, Choi Y, Ruby CL, Oliveros A, Prieto ML, Park JH, Choi DS. 2014; Activation of neurotensin receptor type 1 attenuates locomotor activity. Neuropharmacology. 85 :482–492. [PubMed: 24929110]

van Wimersma Greidanus TB, Schijff JA, Noteboom JL, Spit MC, Bruins L, van Zummeren BM, Rinkel GJ. 1984; Neurotensin and bombesin, a relationship between their effects on body temperature and locomotor activity? Pharmacol Biochem Behav. 21 :197–202. [PubMed: 6483931]

van Zessen R, Phillips JL, Budygin EA, Stuber GD. 2012; Activation of VTA GABA neurons disrupts reward consumption. Neuron. 73 :1184–1194. [PubMed: 22445345]

Volkow ND, Wang GJ, Tomasi D, Baler RD. 2013; The addictive dimensionality of obesity. Biol Psychiatry. 73 :811–818. [PubMed: 23374642]

Voyer D, Levesque D, Rompre PP. 2017; Repeated ventral midbrain neurotensin injections sensitize to amphetamine-induced locomotion and ERK activation: a role for NMDA receptors. Neuropharmacology. 112 :150–163. [PubMed: 27267684]

Watabe-Uchida M, Zhu L, Ogawa SK, Vamanrao A, Uchida N. 2012; Whole-brain mapping of direct inputs to midbrain dopamine neurons. Neuron. 74 :858–873. [PubMed: 22681690]

Werkman TR, Kruse CG, Nievelstein H, Long SK, Wadman WJ. 2000; Neurotensin attenuates the quinpirole-induced inhibition of the firing rate of dopamine neurons in the rat substantia nigra pars compacta and the ventral tegmental area. Neuroscience. 95 :417–423. [PubMed: 10658621]

Woodworth HL, Batchelor HM, Beekly BG, Bugescu R, Brown JA, Kurt G, Fuller PM, Leinninger GM. 2017a; Neurotensin Receptor-1 identifies a subset of ventral tegmental dopamine neurons that coordinates energy balance. Cell Rep. 20 :1881–1892. [PubMed: 28834751]

Woodworth HL, Beekly BG, Batchelor HM, Bugescu R, Perez-Bonilla P, Schroeder LE, Leinninger GM. 2017b; Lateral hypothalamic neurotensin neurons orchestrate dual weight loss behaviors via distinct mechanisms. Cell Rep. 21 :3116–3128. [PubMed: 29241540]

Woulfe J, Beaudet A. 1989; Immunocytochemical evidence for direct connections between neurotensin-containing axons and dopaminergic neurons in the rat ventral midbrain tegmentum. Brain Res. 479 :402–406. [PubMed: 2564307]

Yetnikoff L, Cheng AY, Lavezzi HN, Parsley KP, Zahm DS. 2015; Sources of input to the rostromedial tegmental nucleus, ventral tegmental area, and lateral habenula compared: a study in rat. J Comp Neurol. 523 :2426–2456. [PubMed: 25940654]

Zahm DS, Grosu S, Williams EA, Qin S, Berod A. 2001; Neurons of origin of the neurotensinergic plexus enmeshing the ventral tegmental area in rat: retrograde labeling and in situ hybridization combined. Neuroscience. 104 :841–851. [PubMed: 11440814]

Zahm DS, Cheng AY, Lee TJ, Ghobadi CW, Schwartz ZM, Geisler S, Parsely KP, Gruber C, Veh RW. 2011; Inputs to the midbrain dopaminergic complex in the rat, with emphasis on extended amygdala-recipient sectors. J Comp Neurol. 519 :3159–3188. [PubMed: 21618227]

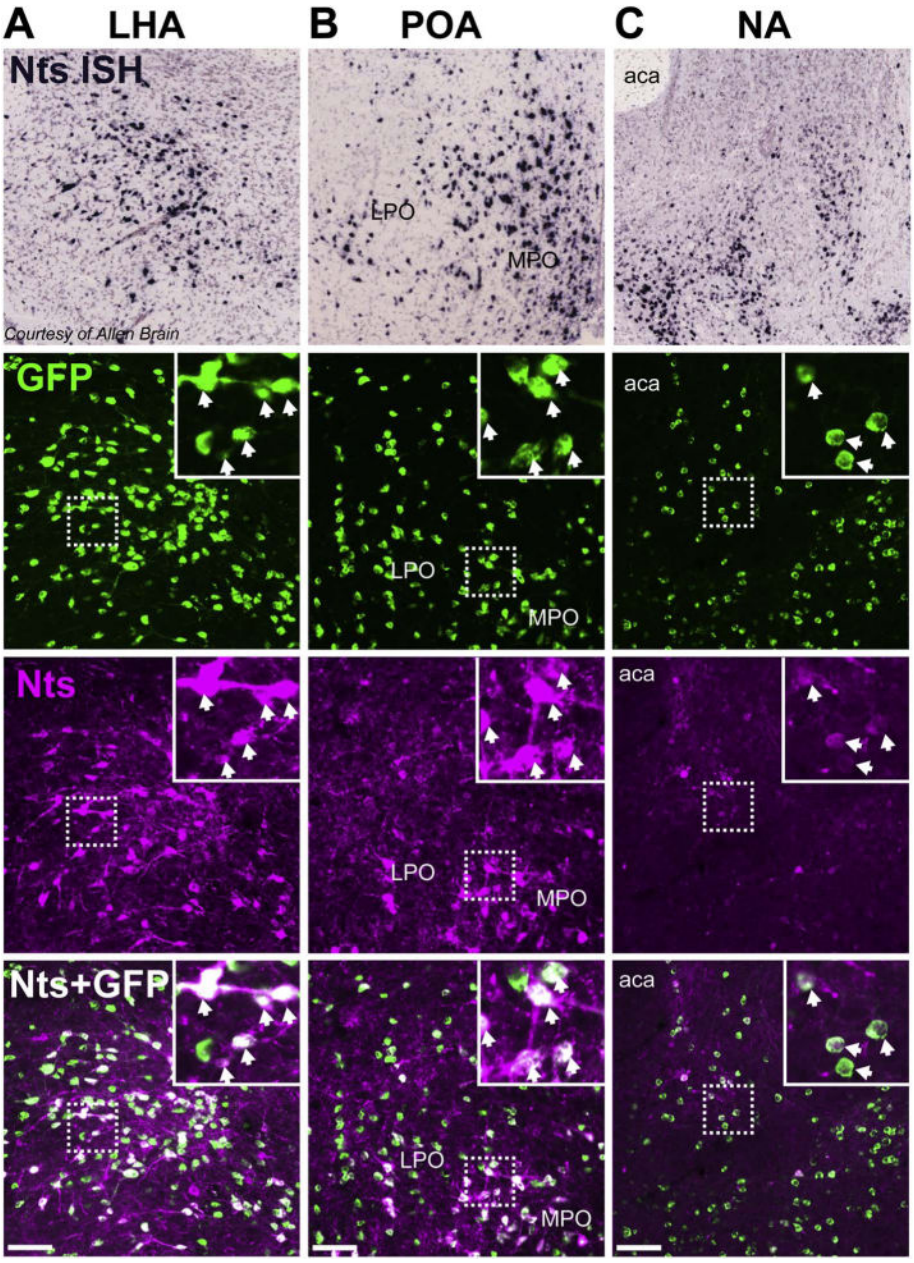

Fig. 1.

Validation of *Nts*^{Cre}*;GFP* mouse model. Side-by-side comparison of Nts mRNA expression via in situ hybridization (ISH) from the Allen Brain Atlas (Lein et al., 2007) to *Nts*^{Cre}*;GFP* mice treated with colchicine and co-stained for Nts peptide using immunofluorescence (magenta). Representative images from the A) LHA, B) POA, and C) NA are shown. Scale bars = 100um. LPO = lateral preoptic area, MPO = medial preoptic area, aca = anterior commissure. (For interpretation of the references to colour in this figure legend, the reader is referred to the web version of this article.)

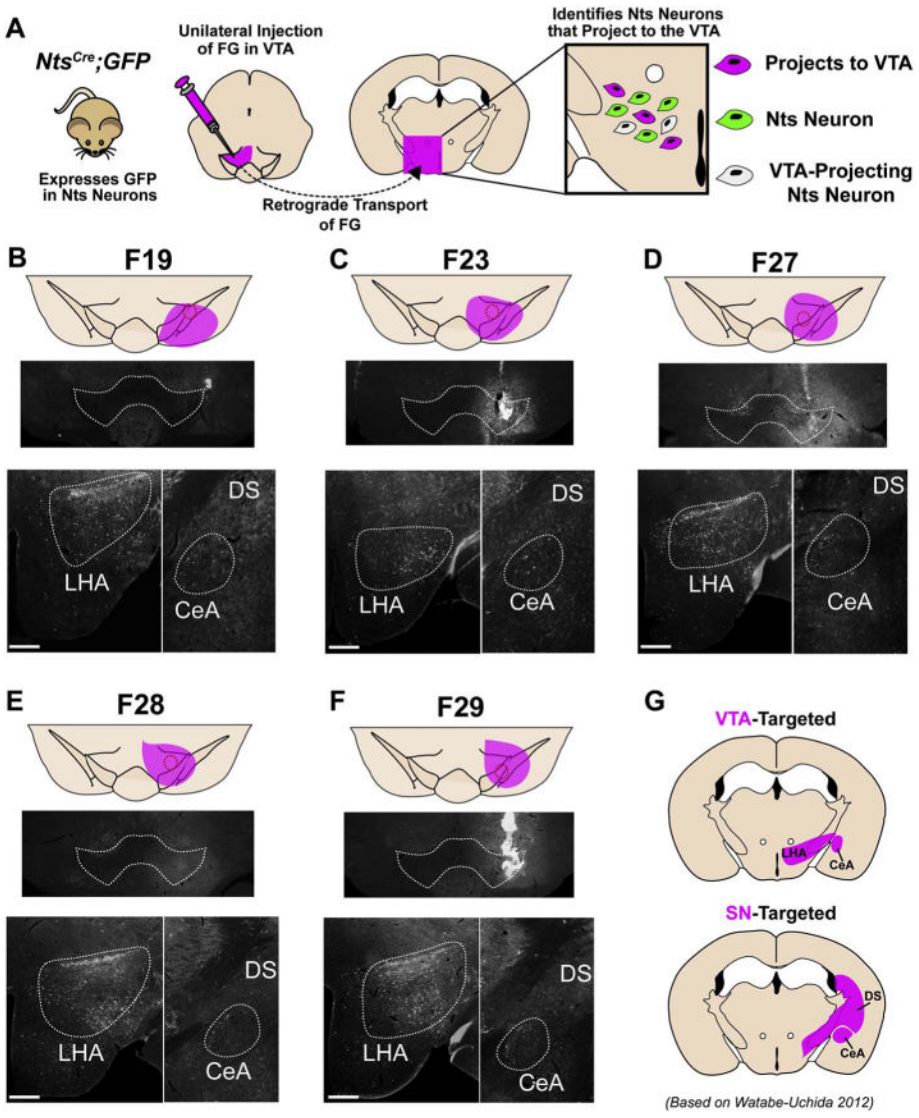

Fig. 2.

Confirmation of VTA targeting in *Nts*^{Cre}*;GFP* mice injected unilaterally with FG. A) *Nts*^{Cre}*;GFP* reporter mice were injected unilaterally in the VTA with FG allowing for simultaneous visualization of neurons that project to the VTA (FG positive neurons), Nts neurons (GFP positive neurons) and Nts afferents to the VTA (GFP/FG+ double-positive neurons). B–F). Midbrain images of the five VTA-targeted *Nts*^{Cre}*;GFP* mice included in the final analysis. The approximate spread of FG is shown in magenta. FG-labeled cell bodies of VTA-targeted animals are confined to the LHA, ZI, CeA, and absent from the DS. G) Expected afferent patterns to the VTA or SN based on Uchida (Watabe-Uchida et al., 2012). Scale bars = 200um. (For interpretation of the references to colour in this figure legend, the reader is referred to the web version of this article.)

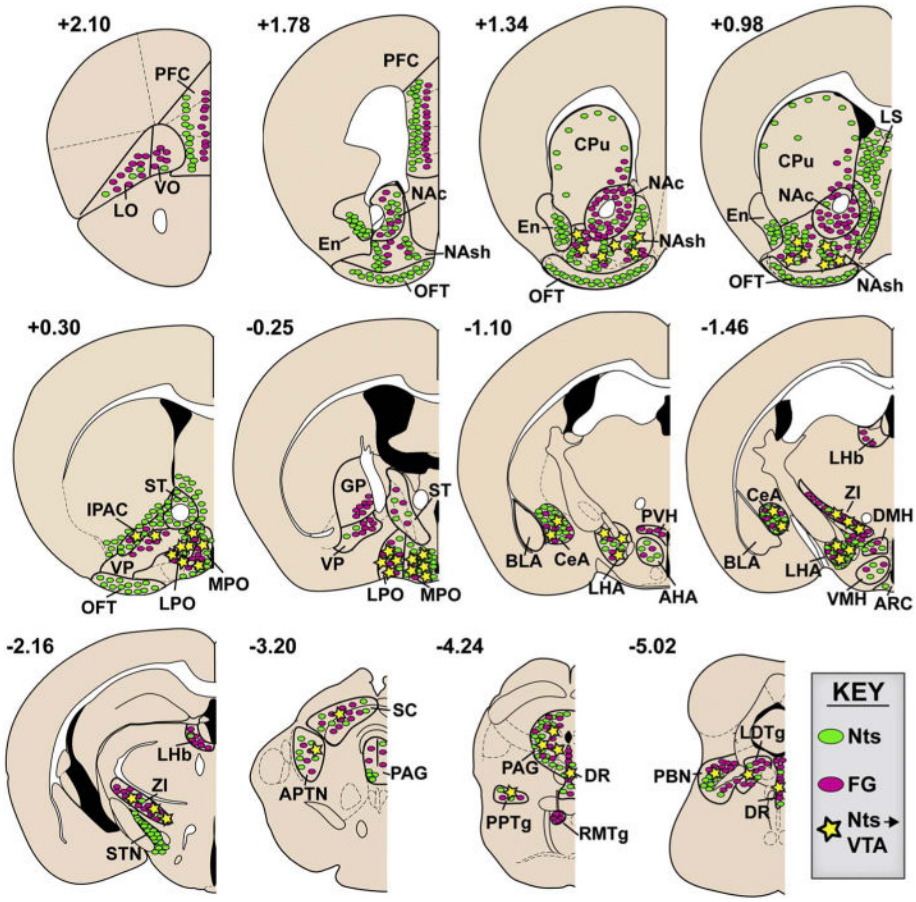

Fig. 3.

Schematic illustration of Nts afferents to the VTA. Distribution patterns of Nts neurons and VTA afferents at different bregma coordinates. Green ovals represent GFP-labeled neurons, pink ovals represent FG-labeled neurons, and yellow stars indicate colocalized Nts/FG+ neurons. Only the sub-regions included in analysis are outlined in black and labeled, and blank regions do not necessarily indicate lack of GFP or FG. (For interpretation of the references to colour in this figure legend, the reader is referred to the web version of this article.)

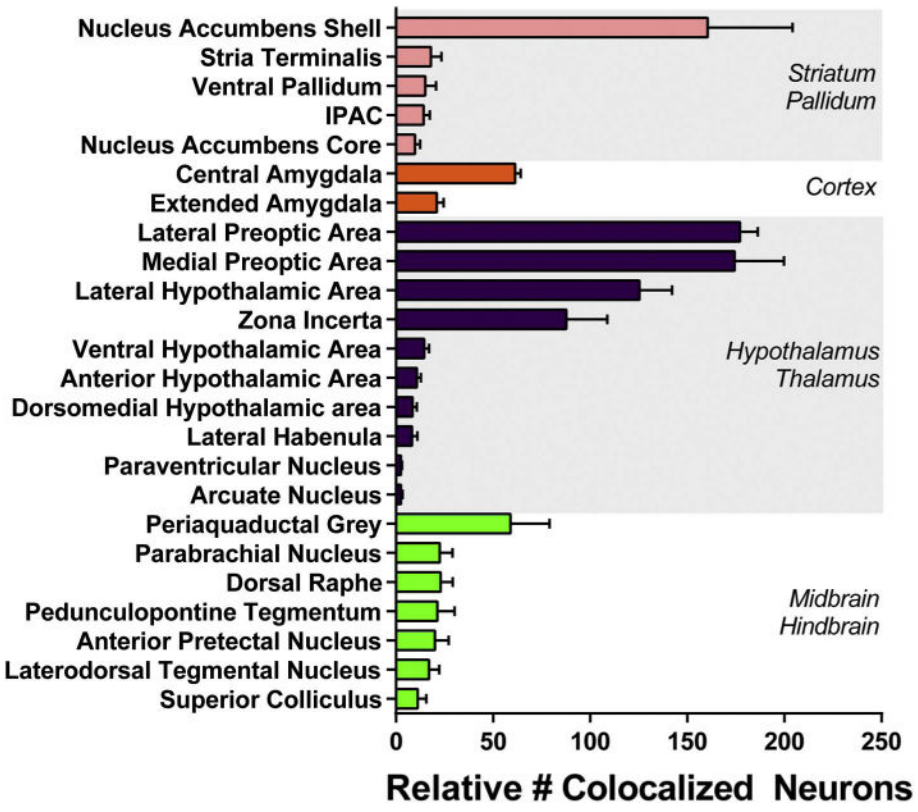

Fig. 4.

Quantification of Nts-expressing afferents to the VTA by anatomical sub-region. Cell bodies colocalized with GFP and FG were counted in one of four coronal series through the brain. Bars thus represent approximately one quarter of the total number of colocalized GFP/FG+ neurons within each region, averaged across all 5 study mice described in Fig. 2B–F. This quantification method is the most conservative method to compare relative neuronal abundance between different brain areas, without oversampling that might occur if the counts were multiplied by 4 to approximate the total number of cells throughout the entire brain region. Areas that contained ≤1 colocalized neuron per section were not included in the quantification.

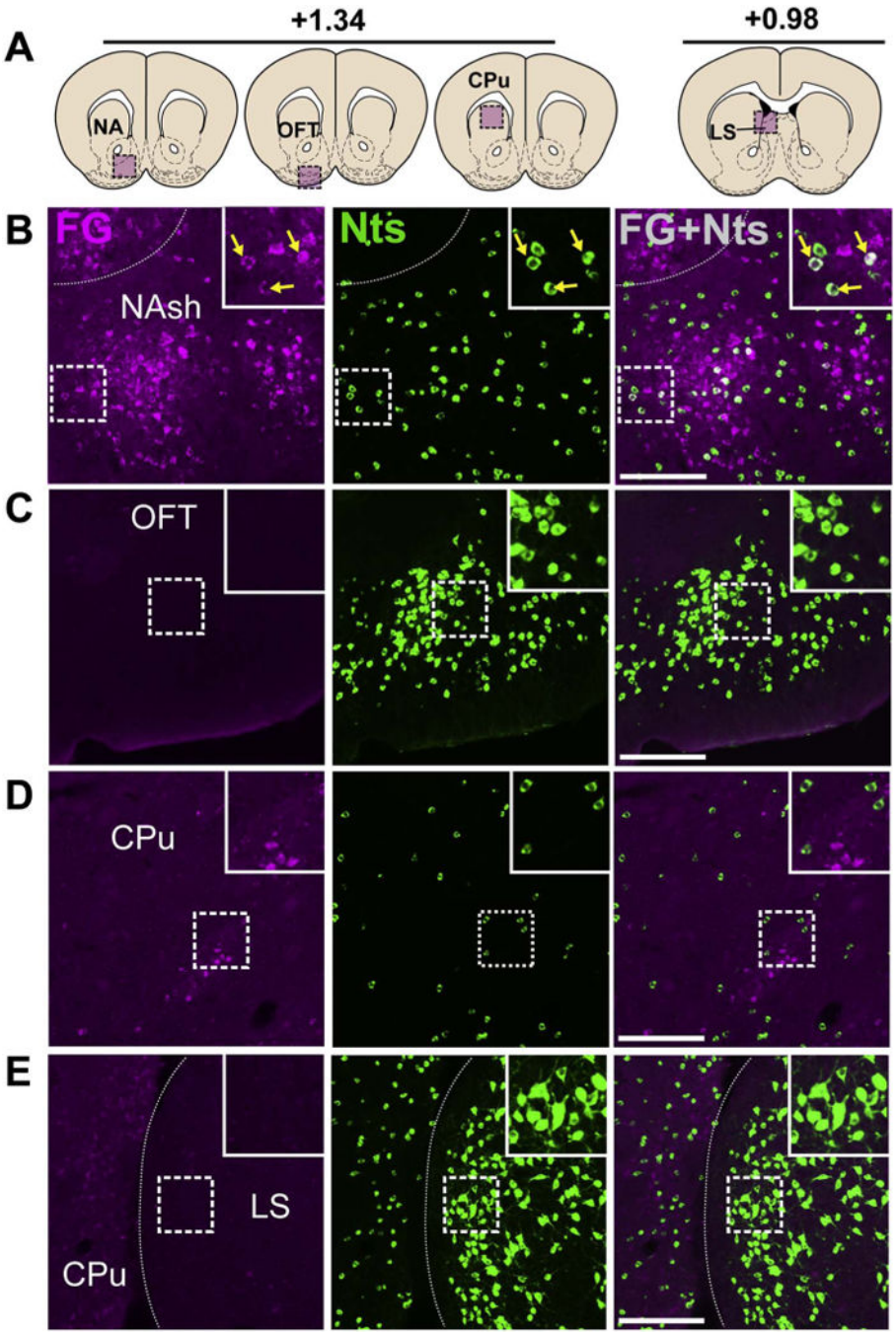

Fig. 5.

The NA shell contains clusters of Nts neurons that project to the VTA. A) Schematic of brain regions analyzed according to distance from Bregma. B) Many Nts/FG+ neurons were found in the NAsh (yellow arrows), but not NAc (Case F19). C) Nts expression in the OFT, an area that does not provide significant VTA input and hence few FG+ neuron was observed (Case F29). D) Representative expression of Nts and FG in the CPu shows little to no colocalization (Case F19). E) Nts neurons were numerous in the LS, an area that does not provide substantial input to the VTA (Case F29). Scale bar = 100uM. NAsh = nucleus

accumbens shell, OFT = olfactory tubercle, CPu = caudate/putamen, LS = lateral septum. (For interpretation of the references to colour in this figure legend, the reader is referred to the web version of this article.)

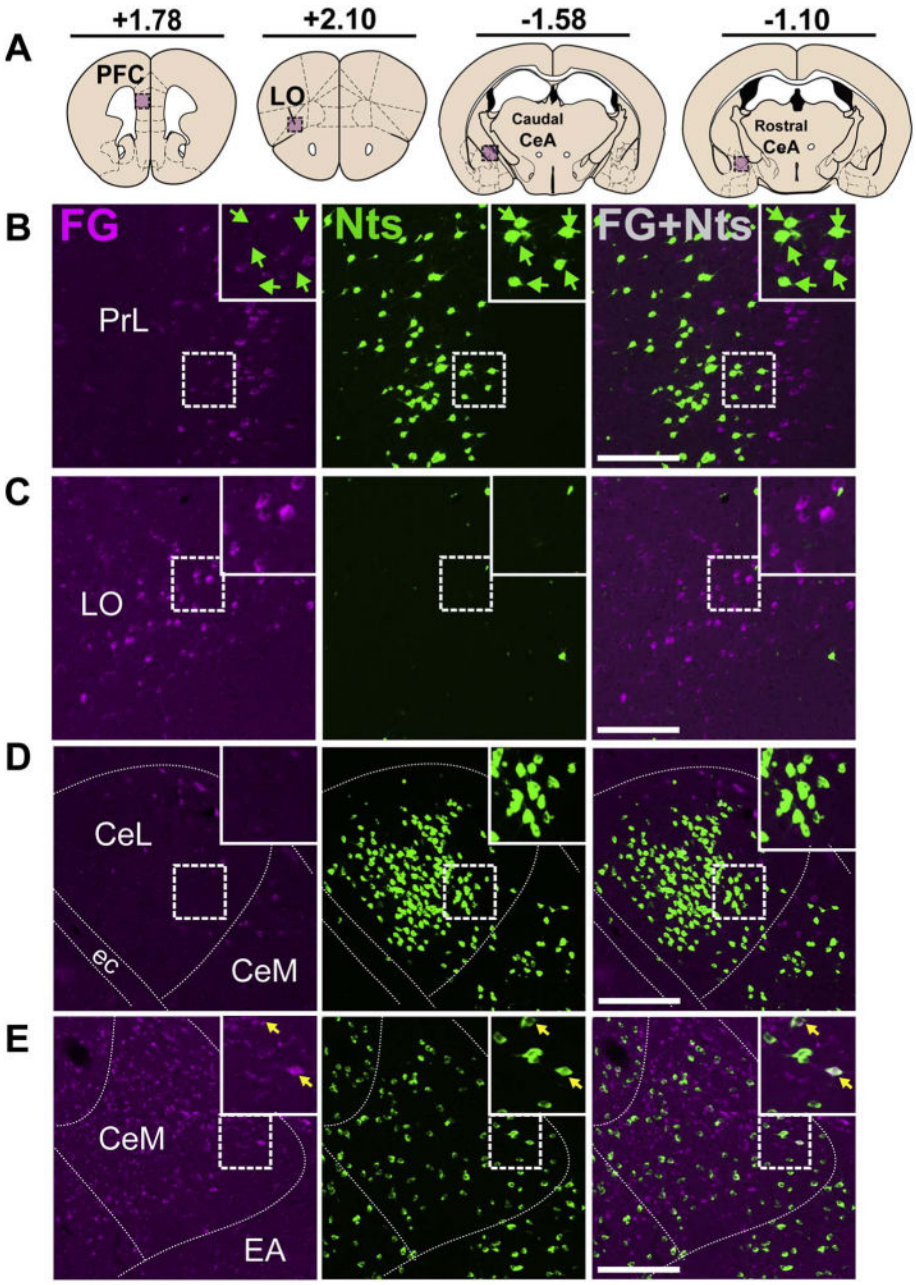

Fig. 6.

Cortical Nts inputs to the VTA originate in the CeA but not neocortex. A). Schematic of brain regions analyzed according to distance from Bregma. Representative images show the absence of FG and Nts co-labeling in the B) PFC and C) LO (Case 27). D) A dense population of Nts neurons resided in the lateral division of the caudal CeA, but these neurons were unlikely to project to the VTA (Case 27). E) Some Nts neurons in the medial CeA project colocalized with FG (yellow arrows) (Case 29). Scale bar = 100um. PrL = prelimbic cortex, LO = lateral orbital cortex CeM = medial division of CeA, CeL = lateral division of CeA, ec = external capsule, EA = extended amygdala. (For interpretation of the

references to colour in this figure legend, the reader is referred to the web version of this article.)

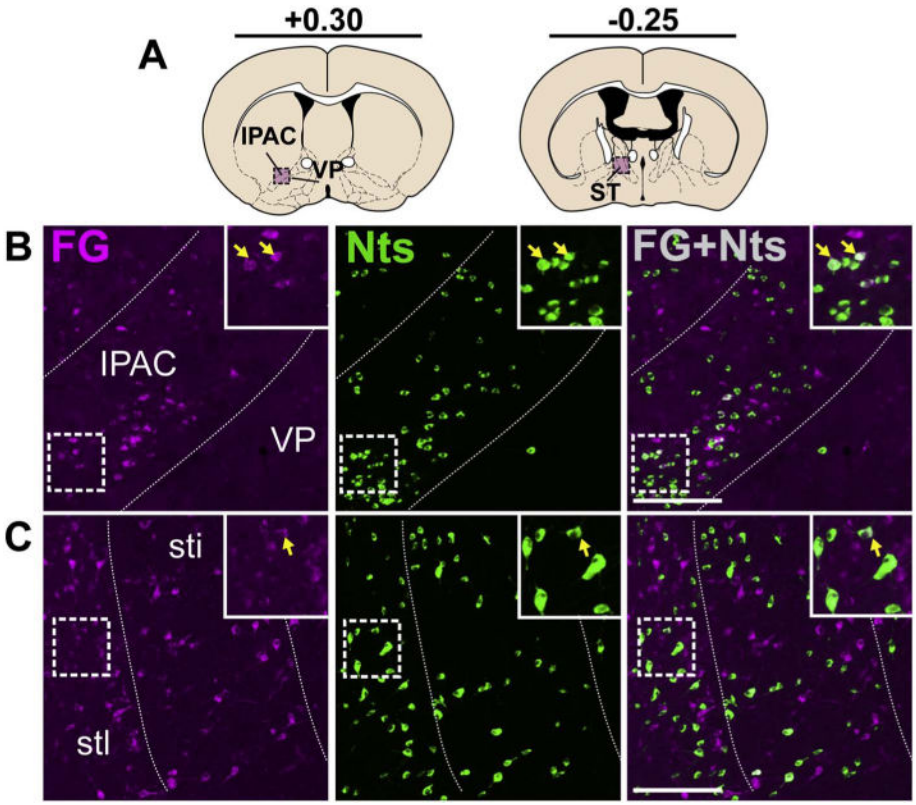

Fig. 7.

Nts neurons in the IPAC, pallidum, and ST that project to the VTA. A) Schematic of brain regions analyzed according to distance from Bregma. B) Nts/FG+ neurons were observed in the lateral IPAC (yellow arrows) while the adjacent VP contained low numbers of Nts neurons (Case F19). C) Nts/FG+ neurons were observed in the ST (yellow arrows) (Case F27). Scale bar = 100um. IPAC = interstitial nucleus of the posterior limb of the anterior commissure, VP = ventral pallidum, stl = lateral division of bed of stria terminalis. (For interpretation of the references to colour in this figure legend, the reader is referred to the web version of this article.)

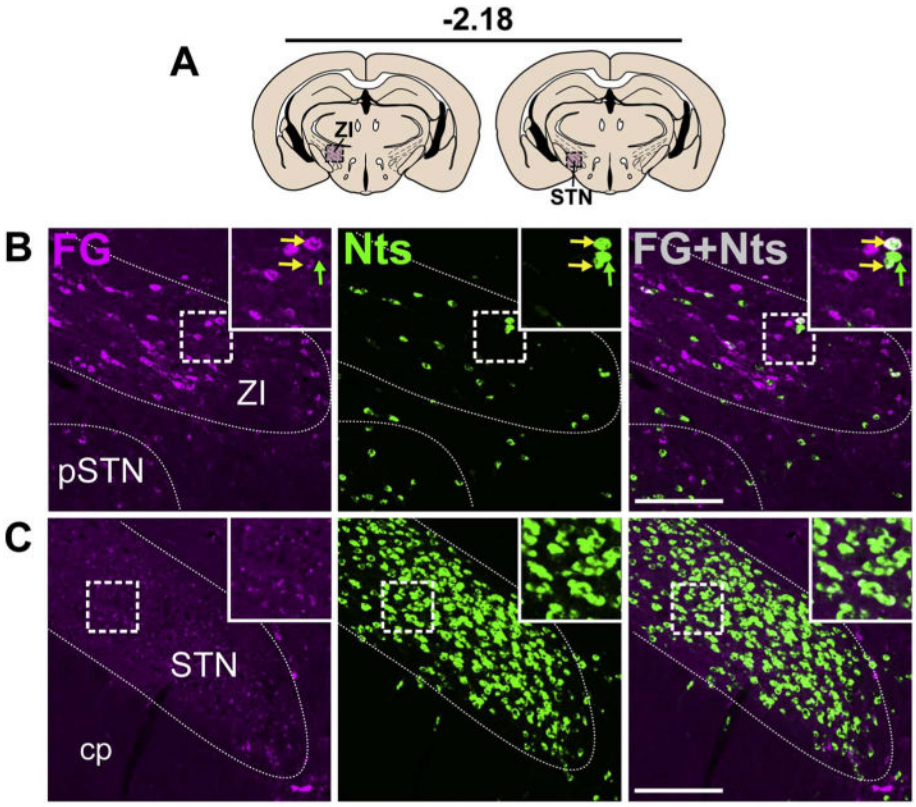

Fig. 8.

Nts-expressing inputs from the ZI and STN. A) Schematic of brain regions analyzed according to distance from Bregma. B) Caudal section of the hypothalamus showing Nts/FG+ neurons in the ZI (yellow arrows) but not the C) STN (both Case F19). Scale bar = 100um. pSTN = para-subthalamic nucleus, ZI = zona incerta, cp = cerebral peduncle. (For interpretation of the references to colour in this figure legend, the reader is referred to the web version of this article.)

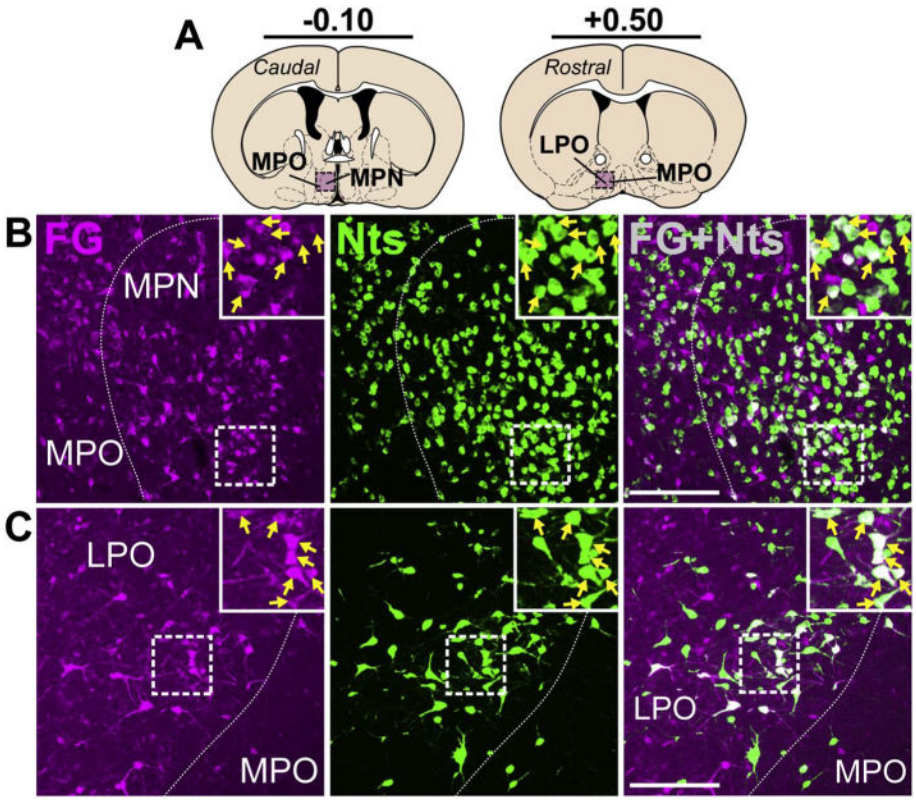

Fig. 9.

Nts projections to the VTA from the POA. A) Schematic of brain regions analyzed according to distance from Bregma. B) A dense Nts population resided in the caudal MPO and many of these were Nts/FG+ neurons that projected to the VTA (yellow arrows) (Case F28). C) Numerous Nts/FG+ neurons were also observed in the rostral LPO (yellow arrows) (Case F23). Scale bars = 100um. MPN = median preoptic nucleus, MPO = medial preoptic area, LPO = lateral preoptic area. (For interpretation of the references to colour in this figure legend, the reader is referred to the web version of this article.)

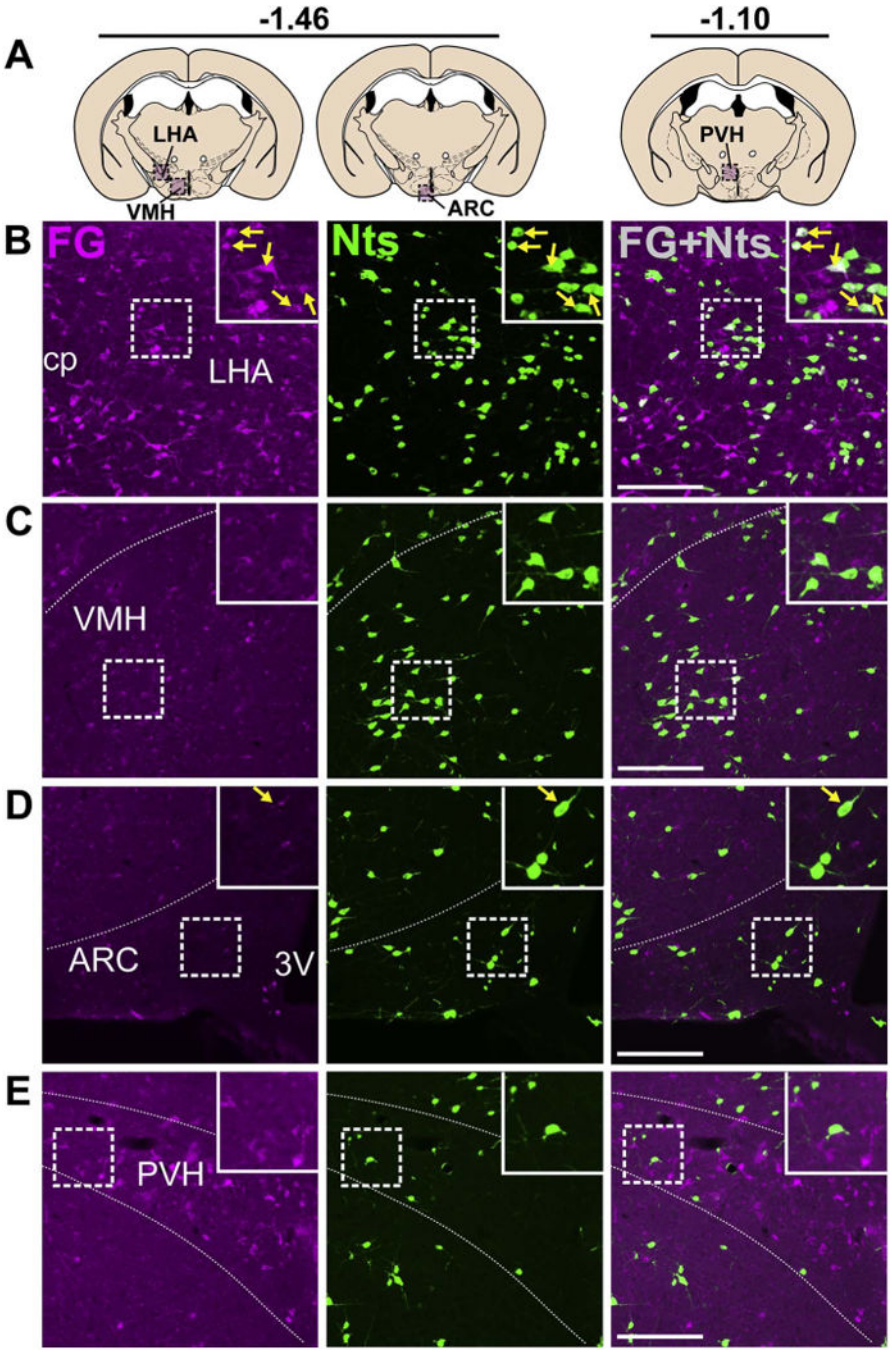

Fig. 10.

Nts inputs from the LHA, VMH, ARC, and PVH. A) Schematic of brain regions analyzed according to distance from Bregma. B) The LHA contained a large number of Nts/FG+ neurons (yellow arrows). C) The VMH and D) ARC did not provide many Nts afferents to the VTA. E) The PVH contained minimal Nts neurons and was not a major source of Nts input to the VTA. All images from Case F28. Scale bars = 100um. cp = cerebral peduncle, LHA = lateral hypothalamic area, VMH = ventromedial hypothalamus, ARC = arcuate nucleus, 3V = third ventricle, PVH = paraventricular hypothalamus. (For interpretation of

the references to colour in this figure legend, the reader is referred to the web version of this article.)

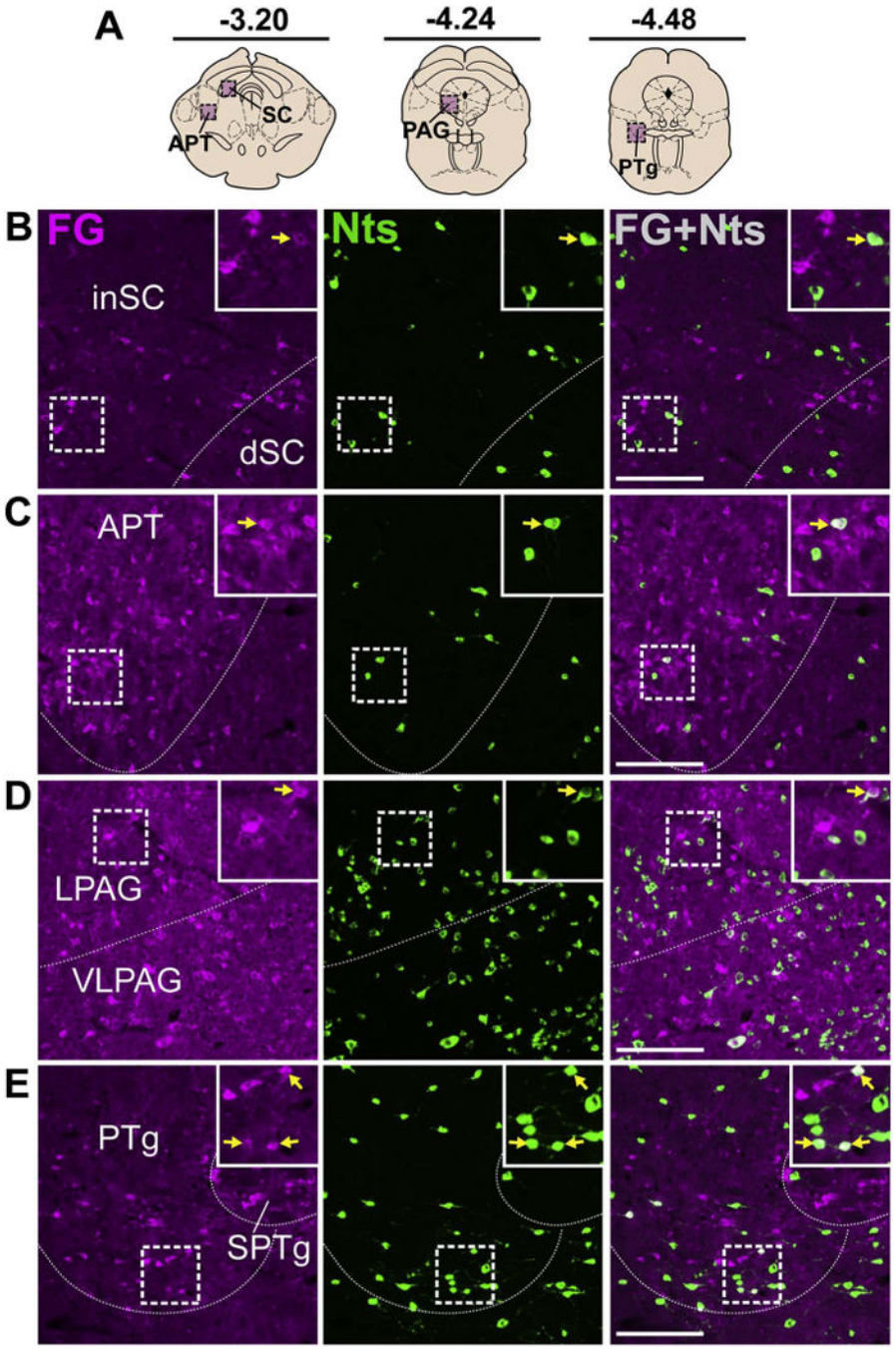

Fig. 11.

Brainstem Nts inputs to the VTA. A) Schematic of brain regions analyzed according to distance from Bregma. Few colocalized neurons were detected in the B) SC, C) APT (both Case F19), D) PAG (Case F27) and E) PTg (Case F19). Scale bar = 100um. inSC = inferior superior colliculus, dSC = dorsal superior colliculus, APT = anterior pretectal nucleus, LPAG = lateral periaqueductal grey, VLPAG = ventrolateral periaqueductal grey, PTg = pedunculopontine tegmental nucleus, SPTg = subpeduncular tegmental nucleus.

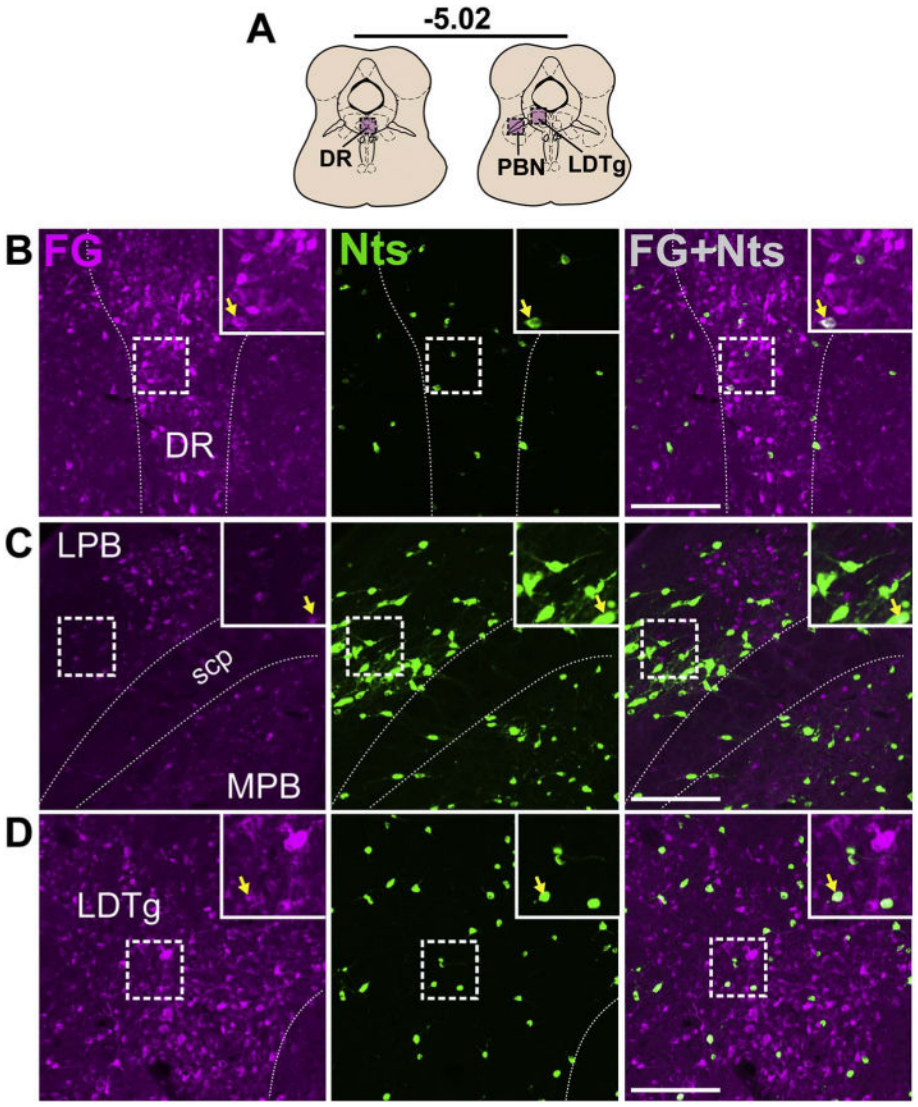

Fig. 12.

Brainstem Nts inputs to the VTA from the DR, PBN, and LDTg. A) Schematic of brain regions analyzed according to distance from Bregma. Few colcoalized neurons were detected in the B) DR, C) PB (both Case F23), and D) LDTg (Case F27). Scale bar = 100um. DR = dorsal raphe, LPB = lateral parabrachial nucleus, MPB = medial parabrachial nucleus, scp = superior cerebellar peduncle, LDTg = laterodorsal tegmental nucleus.

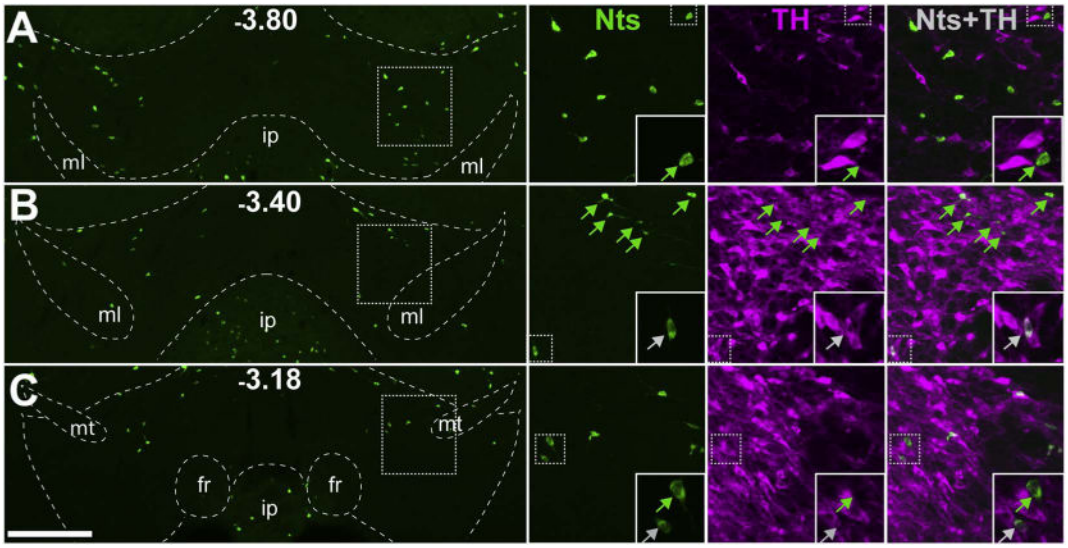

Fig. 13.

Minimal Nts expression in the VTA. *Nts*^{Cre}*;GFP* mice (n = 6) were used to determine the number and distribution of VTA Nts neurons and whether or not they co-express TH. A, B, C) Representative images of GFP-identified Nts neurons across three different bregma coordinates in the VTA of *Nts*^{Cre}*;GFP* mice (scale bar = 200um). Insets highlight individual Nts neurons and the presence or absence of colocalization with TH (greyarrows = TH+ Nts neurons, green arrows = TH- Nts neurons). These data demonstrate that of the few GFP+ cells found in the VTA, the majority do not colocalize with TH and are not DAergic. ml = medial lemniscus, ip = interpeduncular nucleus, fr = fasciculus retroflexus, mt = mammillothalamic tract. (For interpretation of the references to colour in this figure legend, the reader is referred to the web version of this article.)

Table 1

Abbreviations used.

Abbreviation	Full name
3V	Third ventricle
aca	Anterior commissure
AHA	Anterior hypothalamic area
APT	Anterior pretectal nucleus
ARC	Arcuate nucleus
BLA	Basolateral amygdala
CeA	Central amygdala
CeL	Lateral division of the central amygdala
CeM	Medial division of the central amygdala
cp	Cerebral peduncle
CPu	Caudate/putamen
DA	Dopamine
DMH	Dorsomedial hypothalamus
DR	Dorsal raphe
DS	Dorsal striatum
dSC	Dorsal superior colliculus
EA	Extended amygdala
ec	External capsule
En	Entorhinal cortex
FG	Fluoro-Gold
fr	frasiculus retroflexus
GFP	Green fluorescent protein
ip	Interpeduncular nucleus
IPAC	Interstitial nucleus of the posterior limb of the anterior commissure
iSC	Inferior superior colliculus
ISH	in situ hybridization
LDTg	Laterodorsal tegmental nucleus
LHA	Lateral hypothalamic area
LO	Lateral orbital cortex
LPAG	Lateral periaqueductal grey
LPB	Lateral parabrachial nucleus
LPO	Lateral preoptic area
LS	Lateral septum
ml	Medial lemniscus
MPB	medial parabrachial nucleus
MPN	Median preoptic nucleus
MPO	Medial preoptic area
mt	mammillothalamic tract
NA	Nucleus accumbens (all parts)

Abbreviation	Full name
NAsh	Nucleus accumbens shell
Nts	Neurotensin
OFT	Olfactory tubercle
PAG	Periaqueductal grey
PB	Parabrachial nucleus
PFC	Prefrontal cortex
POA	Preoptic area
PrL	Prelimibc cortex
pSTN	Para-substhalamic nucleus
PTg	Pedunculopontine tegmental nucleus
PVH	Paraventricular hypothalamus
RMTg	Rostromedial tegmental nucleus
SC	Superior Colliculus
scp	Superior cerebellar peduncle
SN	Substantia nigra
SPTg	subpeduncular tegmental nucleus
ST	Stria terminalis (general)
sti	Intermediate division of bed of stria terminals
stl	Lateral division of bed of stria terminals
STN	subthalamic nucleus
VLPAG	Ventrolateral periaqueductal grey
VMH	Ventromedial hypothalamus
VO	Ventral orbital cortex
VP	Ventral pallidum
VTA	Ventral tegmental area
ZI	Zona incerta

Table 2

Relative density of Nts afferents to the VTA.

Area	Total # colocalized	# Colocalized per section
LPO	177.2 ± 9.1	32.1 ± 2.7
MPO	174.4 ± 25.4	31.7 ± 5.2
LHA	125.4 ± 18.7	22.3 ± 2.9
NAsh	160.5 ± 43.8	19.2 ± 5.9
ZI	87.8 ± 21.1	8.6 ± 2.3
CeA	61.3 ± 2.9	8.5 ± 0.1
PAG	59.0 ± 20.0	3.8 ± 1.6